International Journal of Steel Structures 17(2): 443-469 (2017)
DOI 10.1007/s13296-017-6006-8
ISSN 1598-2351 (Print)
ISSN 2093-6311 (Online)

International Journal of
STEEL
STRUCTURES
www.springer.com/journal/13296

Structural Stability of Cable-stayed Bridges during Construction

Hong-Jung Kim[1], Deok Hee Won[2], Young-Jong Kang[3], and Seungjun Kim[4,*]

[1]*Senior researcher, Korea Agency for Infrastructure Technology Advancement, Anyang, Korea*
[2]*Senior Research Scientist, Ph.D., Coastal & Environmental Engineering Division, Korea Institute of Ocean Science and Technology, Ansan, Korea*
[3]*Professor, Ph.D., School of Architectural, Civil and Environmental Engineering, Korea University, Seoul, Korea*
[4]*Assistant professor, Ph.D., Department of Construction Safety and Disaster Prevention Engineering, Daejeon University, Daejeon, Korea*

Abstract

This paper presents an investigation of the stability characteristics of steel cable-stayed bridges during construction. In general, cable-stayed bridges are subjected to quite large compressive forces induced by stayed cables, and may become unstable during their construction stage, due to the excessive compressive forces induced by added construction loads. To solve the structural instability problems of the bridges under construction, a nonlinear analysis program was developed based on the theory of nonlinear finite element analysis. The complex stability characteristics of cable-stayed bridges during construction were investigated through a series of rigorous geometric nonlinear analyses, including various structural nonlinearities such as cable-sag effect, beam-column effect of girder and mast, large displacement effect, and girder-mast-cable interaction. To consider the construction characteristics of the cable-stayed bridges, a three-step analysis method is proposed, and used in the present study. In addition, the effects of various cable-arrangement types and girder-mast stiffness ratios on the stability characteristics were extensively investigated. Typical buckling modes can be classified into two categories, depending on the location of critical member or members.

Keywords: cable-stayed bridges, nonlinear analysis, initial shape analysis, construction stage analysis, generalized displacement control method

1. Introduction

The cable-stayed bridge has become the most popular bridge system because of its structural efficiency and pleasing aesthetics. The structural system of the cable-stayed bridge consists of girder, mast and cables. Among these main members, stay cables are considered as intermediate supports of the girder. So, cable-stayed bridges are suitable for long-span bridges with suspension bridges.

It is well known that cable-stayed bridges exhibit complex nonlinear characteristics (Adeli and Zhang, 1994; Xi and Kuang, 1999; Ren, 1999; Freire *et al.*, 2006). The following factors lead to the nonlinear behavior of cable-stayed bridges. The first is the cable-sag effect initiated by its own weight. The second is the beam-column effect of the girder and mast. The girder and mast of cable-stayed bridges are subjected to large compressive forces induced by tensile forces of the stay cables. The applied compressive force amplifies the flexural behavior of girder and mast, so it results in a beam-column effect. Also, the large displacement or deformation effect produced by geometric change of the structure leads to geometric nonlinear behavior. Furthermore, the girder-mast-cable interaction affects the complex nonlinear behavior. When external load is applied to the girder first, it is transferred to the mast by stayed cables, because these connect the girder and mast. Because of the connection between the main members, the local structural behavior of each member affects the behavior of other members, which may result in global behavior and global changes of structural state.

Stay cables are designed as intermediate support members of the girder. The vertical components of tensile forces of cables are hanging on the girder. So, more tensile forces are needed to support the girder and to resist applied vertical loads. But compressive forces applied to the girder and mast increase as tensile forces of cables increase, because of the structural characteristics of cable-stayed bridges. This is significantly different behavior to that of suspension bridges. Because stay cables are directly connected to both girder and mast, vertical and horizontal components of tensile forces are directly applied to the

Received April 20, 2016; accepted October 9, 2016;
published online June 30, 2017
© KSSC and Springer 2017

*Corresponding author
Tel: +82-42-280-4574, Fax: +82-42-280-2576
E-mail: skim@dju.kr

mast and girder as compressive forces. Therefore, problems of structural instability may occur as external forces increase, because compressive forces applied to the girder and mast increase also. In general, members subjected to compressive forces may buckle and the structure may become unstable. Buckling of the mast or girder means that the structure reaches a critical state. Therefore, the characteristics of structural stability of cable-stayed bridges should be studied, because the main members of cable-stayed bridges are always subject to quite large compressive forces, due to inclined cables. In addition, buckling analysis for cable-stayed bridges should be performed by rational analysis method based on the theory of nonlinear finite element analysis, because of the various nonlinear factors.

Studies to investigate the characteristics of structural stability or ultimate behavior of completed cable-stayed bridges have been performed. Researches have been performed to investigate the structural stability of completed cable-stayed bridges using eigenvalue analysis (Tang *et al*., 2001; Shu and Wang, 2001). In these studies, various buckling modes were introduced, and the effects of various geometric properties on the structural stability were described. But various nonlinearity factors were not considered in these studies, because they were conducted by conventional eigenvalue analyses. Furthermore, the initial condition, which can be considered by initial shape analysis, was not considered before considering the live load condition. This is very important, because cable-stayed bridges are designed with optimal initial tensile forces of cables, which make for minimum deformation and internal forces under dead load condition (Chen *et al*., 2000; Cheng and Xiao, 2007; Kim and Lee, 2001; Wang *et al*., 1993; Wang and Yang, 1993).

Eigenvalue analysis is not suitable for stability analysis of cable-stayed bridges for the following critical reasons. A. Typical eigenvalue analysis cannot consider nonlinearities, because eigenvalue analysis is basically a type of linear elastic analysis (Adeli and Zhang, 1993; Wang and Yang, 1995; Xi and Kuang, 1999; Ren, 1999; Freire *et al*., 2006; Kim *et al*., 2015). B. It is difficult to reflect the structural state under dead load condition, before buckling analysis under various live load cases. Therefore, it is clear that nonlinear analysis should be performed as the buckling analysis for cable-stayed bridges. Some studies using nonlinear analysis have been performed. Song and Kim (2007) used a nonlinear analysis method for obtaining the ultimate capacity of cable-stayed bridges, and suggested ultimate analysis method considering geometric and material nonlinearities. Their study focuses on the ultimate capacity of completed cable-stayed bridges. Ren (1999) also studied the ultimate behavior of completed cable-stayed bridges. That study considers the ultimate behavior and capacity of concrete cable-stayed bridges by considering various nonlinearities, boundary conditions, and loading conditions. Kim *et al*. (2015) studied the structural stability of the cable-stayed bridges considering the initial stage force-equilibrium condition. In the study, various structural instability modes and characteristics were presented based on the intensive nonlinear numerical simulation results. But the study also focuses on the behavior of completed bridges. Lee *et al*. (2015) presented the experimental study of the steel cable-stayed bridges before closing stage. In this study, ultimate behavior of the scaled models were investigated. But, the study was conducted for very limited cases experimentally. In summary, the ultimate behavior or structural stability of cable-stayed bridges under construction has not been actively studied.

It can be said that cable-stayed bridges under construction are more structurally unstable than the completed structure, because of the characteristics of the general construction method. Figure 1 shows the general construction stages and method, using the FCM (free cantilever method) method. As shown in this figure, cable-stayed bridges during the construction stage have more unstable boundary conditions than the completed structure. After completing the construction, through the erection of the key segment of the girder, each part of the cable-stayed bridge is connected with each other part, so they are closed and share the boundary conditions. But, before the closing and connection of two parts constructed individually, each part is supported by more unstable boundary conditions than the completed structure. Therefore, the structural stability each stage of the construction should be analyzed and considered.

Research into the structure of cable-stayed bridges under construction has been performed. But those studies focus on the development of a rational construction stage analysis method (Reddy *et al*., 1999; Wang *et al*., 2004). Through construction stage analysis, the general behavior of the cable-stayed bridge under construction has been studied, such as the characteristics of internal force distributions, structural deformations and so on. But the structural stability of cable-stayed bridges during the construction stage has not been studied.

In this analytical study, characteristics of the cable-stayed bridge under construction are investigated. To perform rational buckling analysis, a nonlinear analysis program for cable-stayed bridges is first developed based on the theory of nonlinear finite element analysis. A three-step analysis method is suggested, in order to consider the characteristics of the design and construction method of cable-stayed bridges. Using this program, intensive analytical study is performed to investigate the structural stability of cable-stayed bridges under construction, especially for the construction stage before the connection of two individual parts. By this analytical study, the governing elastic buckling modes are classified into two categories. Furthermore, the effect of geometric properties on the structural stability is studied, such as cable arrangement type and girder-mast stiffness ratio.

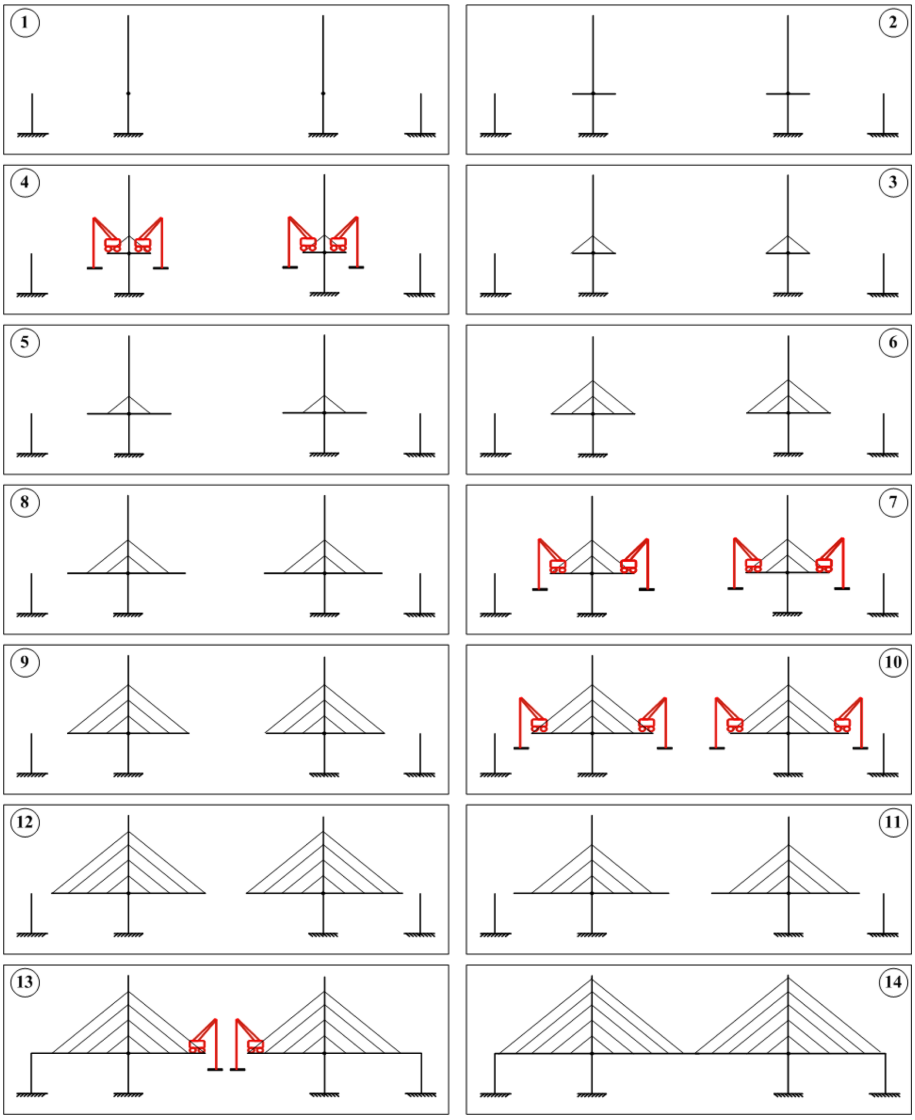

Figure 1. General FCM construction procedure for cable-stayed bridges.

2. Theoretical Background

Because cable-stayed bridges have various nonlinear factors, conventional eigenvalue analysis is not rational for elastic buckling analysis. For elastic buckling analysis of cable-stayed bridges, the cable-sag effect, beam-column effect, large displacement effect and girder-mast-cable interaction should be considered using a rational method. Therefore, geometric nonlinear analysis should be adopted for elastic buckling analysis. For elastic buckling analysis of cable-stayed bridges subject to external forces, other analyses are needed in addition to nonlinear analysis under external loads. Because of the characteristics of design and construction, the initial shape analysis and construction stage analysis should be performed before the external load analysis. Cable-stayed bridges are designed with optimal cable tensile forces, causing the girder and mast to suffer minimum deformation under the dead load condition, thus minimal bending moments occur at the girder and mast. This structural state can be obtained by performing initial shape analysis, a type of special analysis method for cable-stayed bridges.

In addition, construction stage analysis also should be considered for rational analytical study. At every construction stage, the structural states of cable-stayed bridges are different. So, construction stage analysis should be performed before external load analysis to consider the structural state rationally under construction.

In this chapter, the theoretical background of the developed program is described. Nonlinear elements for modeling girder, mast and cable are first introduced. Then, the incremental-iterative analysis scheme for tracing the nonlinear response is introduced. Finally, the proposed elastic buckling analysis method for cable-stayed bridges under construction is described.

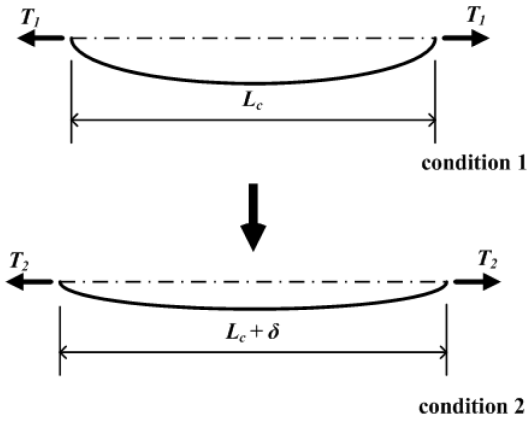

Figure 2. Two conditions for a horizontal stay cable with tensile forces T_1 and T_2, respectively (Gimsing, 1983; Kim *et al.*, 2015)

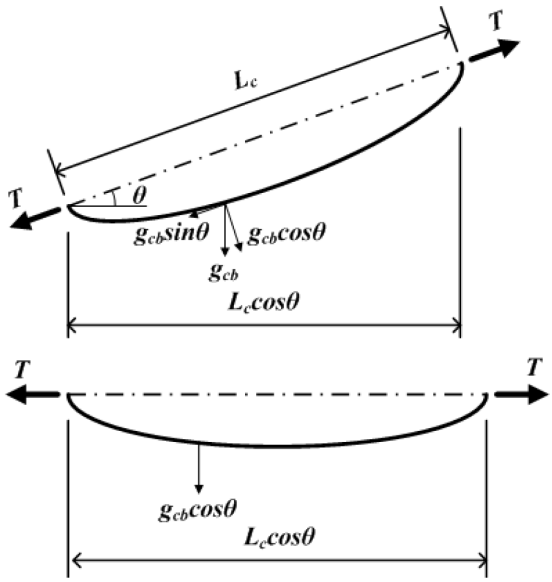

Figure 3. Inclined stay cable and equivalent horizontal stay cable with equal deformational characteristics. g_{cb}: weight per unit length of a cable, T: tensile force (Gimsing, 1983; Kim *et al.*, 2015)

2.1. Cable element

Stayed cable can be modelled by the nonlinear equivalent truss element. The equivalent truss element is a modified truss element that uses an equivalent elastic modulus in order to consider the sag effect of the cable. Figure 2 shows the change of the structural condition due to the tension change, and Fig. 3 shows configurations of the inclined stay cables.

The nonlinear truss element has 2 nodes and 3 degrees of freedom. Equation (1) shows the elastic stiffness and geometric stiffness of the nonlinear element. As shown in the equation, the equivalent elastic modulus is adopted in order to consider the cable-sag effect defined by the weight and tensile force of a cable member. The equivalent modulus, the tangential or secant modulus calculated by the equation for considering cable-sag effect, replaces the conventional elastic modulus of the truss element (Ernst, 1965; Fleming, 1979; Gimsing, 1983). Consequently, the stiffness matrix could be written by using the tangential or secant elastic modulus as follow (Kim *et al.*, 2015):

$$[k]=[k_e]+[k_g]=\frac{{}^1E_{eq}+{}^1A}{{}^1L_c}\begin{bmatrix}1&0&0&-1&0&0\\&0&0&0&0&0\\&&0&0&0&0\\&&&1&0&0\\&&&&0&0\\&&&&&0\end{bmatrix}+\frac{{}^1\tau_{11}\,{}^1A}{{}^1L_c}\begin{bmatrix}1&0&0&-1&0&0\\&1&0&0&-1&0\\&&1&0&0&-1\\&&&1&0&0\\&&&&1&0\\&&&&&1\end{bmatrix} \quad (1)$$

where

$[k]$ =stiffness matrix of a nonlinear equivalent truss element
$[k_e]$ =elastic stiffness matrix
$[k_g]$ =geometric stiffness matrix
${}^1E_{eq}$ ={}^1E_{tan} or ${}^1E_{sec}$
${}^1E_{tan}$ =tangential modulus
${}^1E_{sec}$ =secant modulus
${}^1\tau_{11}$ =axial stress of a cable member
${}^1A$ =sectional area of a cable member
${}^1L_c$ =length of a cable members

In the Eq. (1), Left superscript refers to the occurring configurations as below: 0=initial undeformed configuration, 1=last known deformed configuration, 2=current deformed configuration. The terms without any superscript such as elastic modulus E are those at the initial undeformed configuration. Also, every terms with superscript 1 are those at the current configuration, so they are updated at every incremental-iterative steps in order to obtain the

physical terms at the current deformed configuration.

In this study, the equivalent elastic modulus directly derived from the shape function of elastic catenary is used for the stiffness matrix of the cable member. The equation for the equivalent elastic modulus is as follows (Song *et al*., 2006; Kim *et al*., 2015):

$$E_{\tan} = \frac{E}{(1+K_1+K_2)/2\cosh\left(\frac{g_{cb}L_c\cos\theta}{2T_i}\right)} \tag{2}$$

where

$$K_1 = \frac{1}{g_{cb}\cdot L_c\cos\theta}\left[2T_i\sinh\left(\frac{g_{cb}\cdot L_c\cos\theta}{T_i}\right) - g_{cb}\cdot L_c\cos\theta\cdot\sinh\left(\frac{g_{cb}\cdot L_c\cos\theta}{T_i}\right)\right]$$

$$K_2 = \frac{-4EA}{g_{cb}\cdot L_c\cos\theta}\left[\sinh\left(\frac{g_{cb}\cdot L_c\cos\theta}{2T_i}\right) - \frac{g_{cb}\cdot L_c\cos\theta}{2T_i}\cdot\cosh\left(\frac{g_{cb}\cdot L_c\cos\theta}{2T_i}\right)\right]$$

$$E_{\sec} = \frac{(T_f - T_i)}{\frac{\delta}{c}} = \frac{E}{(1+K_1+K_2)/2\cosh\left(\frac{g_{cb}\cdot L_c\cos\theta}{2T_f}\right)} \tag{3}$$

where

$$K_1 = \frac{1}{g_{cb}\cdot L_c\cos\theta(T_f - T_i)}\left[T_f^2\sinh\left(\frac{g_{cb}\cdot L_c\cos\theta}{T_f}\right) - T_i^2\sinh\left(\frac{g_{cb}\cdot L_c\cos\theta}{T_i}\right)\right]$$

$$K_3 = \frac{4EA}{g_{cb}\cdot L_c\cos\theta(T_f - T_i)}\left[T_i\sinh\left(\frac{g_{cb}\cdot L_c\cos\theta}{2T_i}\right) - T_f\sinh\left(\frac{g_{cb}\cdot L_c\cos\theta}{2T_f}\right)\right]$$

g_{cb} =weight per unit length of the cable
T_i =tensile force at condition 1
T_f =tensile force at condition 2
$L_c\cos\theta$ =horizontally projected length of the cable

2.2. Nonlinear frame element

The girder and mast of cable-stayed bridges, subjected to compressive force while bending behavior occurs, are modelled by the nonlinear frame element derived by an updated Lagrangian formulation. Figure 4 presents the nodal displacements and forces of the nonlinear frame element used in this study. In the derived procedure of the stiffness matrix, the high order terms of the strain are considered and the additional induced stiffness matrix is adopted as well as the elastic and geometric stiffness matrix of the nonlinear frame element (Yang and Kuo, 1994; Lim *et al*., 2008; Kim *et al*., 2015).

The Eqs. (4)~(6) describe the stiffness matrix composed of elastic, geometric and induced stiffness matrix (Yang and Kuo, 1994; Lim *et al*., 2008; Kim *et al*., 2015).

$$[k] = [k_e] + [k_g] + [k_i] \tag{4}$$

where

$[k_e]$ =elastic stiffness matrix
$[k_g]$ =geometric stiffness matrix
$[k_i]$ =induced stiffness matrix

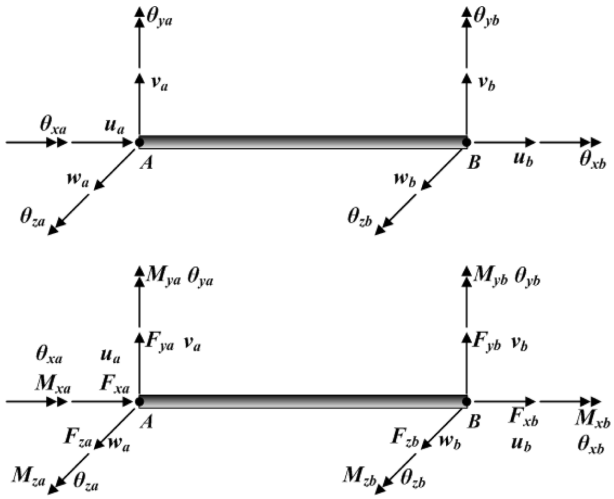

Figure 4. Nodal displacements and forces of the nonlinear frame element.

$$[k_g]=\begin{bmatrix} a & 0 & 0 & 0 & -d & -e & -a & 0 & 0 & 0 & -n & -o \\ & b & 0 & d & g & k & 0 & -b & 0 & n & -g & k \\ & & c & e & -h & g & 0 & 0 & -c & o & -h & -g \\ & & & f & i & l & 0 & -d & -e & -f & -i & -l \\ & & & & j & 0 & d & -g & h & -i & p & -q \\ & & & & & m & e & -k & -g & -l & q & r \\ & & & & & & a & 0 & 0 & 0 & n & o \\ & & & & & & & b & 0 & -n & g & -k \\ & & & & & & & & c & -o & h & g \\ & & & & & & & & & f & i & l \\ & & & & & & & & & & j & 0 \\ & & & & & & & & & & & m \end{bmatrix} \quad (5)$$

where

$$a=\frac{{}^1F_{xb}}{{}^1L},\ b=\frac{6{}^1F_{xb}}{5{}^1L}+\frac{12{}^1F_{xb}I_z}{A{}^1L^3},\ c=\frac{6{}^1F_{xb}}{{}^1L}+\frac{12{}^1F_{xb}I_y}{A{}^1L^3},$$

$$d=\frac{{}^1M_{ya}}{{}^1L},\ e=\frac{{}^1M_{za}}{{}^1L},\ f=\frac{{}^1F_{xb}J}{A{}^1L},\ g=\frac{{}^1M_{xb}}{{}^1L},$$

$$h=\frac{{}^1F_{xb}}{10}+\frac{6{}^1F_{xb}I_y}{A{}^1L^2},\ i=\frac{{}^1M_{za}+{}^1M_{zb}}{6},$$

$$j=\frac{2{}^1F_{xb}{}^1L}{15}+\frac{4{}^1F_{xb}I_y}{A{}^1L},\ k=\frac{{}^1F_{xb}}{10}+\frac{6{}^1F_{xb}I_z}{A{}^1L^2},$$

$$l=\frac{{}^1M_{ya}+{}^1M_{yb}}{6},\ m=\frac{2{}^1F_{xb}{}^1L}{15}+\frac{4{}^1F_{xb}I_z}{A{}^1L},$$

$$n=\frac{{}^1M_{yb}}{{}^1L},\ o=\frac{{}^1M_{zb}}{{}^1L},\ p=\frac{{}^1F_{xb}{}^1L}{30}+\frac{2{}^1F_{xb}I_y}{A{}^1L},$$

$$q=-\frac{{}^1M_{xb}}{2},\ r=-\frac{{}^1F_{xb}{}^1L}{30}+\frac{2{}^1F_{xb}I_z}{A{}^1L}$$

A =sectional area of the frame element
L =length of the frame element
I_y, I_z =2nd moment of inertia with respect to the y and z axis, respectively
J =torsional constant

$$[k_i]=\begin{bmatrix} [0] & & & \\ & [k_i]_a & & \\ & & [0] & \\ & & & [k_i]_b \end{bmatrix} \quad (6)$$

where

$$[k_i]_a=\begin{bmatrix} 0 & 0 & 0 \\ {}^1M_{za} & 0 & -{}^1M_{xa}/2 \\ -{}^1M_{ya}/2 & {}^1M_{xa}/2 & 0 \end{bmatrix}$$

$$[k_i]_b=\begin{bmatrix} 0 & 0 & 0 \\ {}^1M_{zb} & 0 & -{}^1M_{xb}/2 \\ -{}^1M_{yb}/2 & {}^1M_{xb}/2 & 0 \end{bmatrix}$$

2.3. Incremental-iterative analysis scheme

In order to trace nonlinear response, a rational and effective incremental-iterative solving strategy should be considered. Such analysis schemes can be classified into several categories, including the force-control method, displacement-control method and work control method. In general, the Newton-Rapshon method, a type of force-control method, is widely used for the numerical scheme of the nonlinear problem. However, this method is not suitable for nonlinear analysis of a structure that shows complex nonlinear behavior and structurally unstable states, because changeable load factors cannot be considered.

In this study, the generalized displacement control method (Yang and Kuo, 1994; Lim *et al*., 2008; Kim *et al*., 2015) is adopted for incremental-iterative analysis method. The Eqs. (7) and (8) are used for determination of the incremental-iterative load factor at each analysis step.

$$\lambda_1=\pm\lambda_1^1|GSP|^{1/2} \quad (j=1) \quad (7)$$

$$\lambda_j=\frac{\{\Delta\hat{U}_1^{i-1}\}^T\{\Delta\overline{U}_j\}}{\{\Delta\hat{U}_1^{i-1}\}^T\{\Delta\hat{U}_j\}} \quad (j\geq 2) \quad (8)$$

where

$GSP=\dfrac{\{\Delta\hat{U}_1\}^T\{\Delta\hat{U}_1^1\}}{\{\Delta\hat{U}_1^{i-1}\}^T\{\Delta\hat{U}_1\}}$, Generalized stiffness parameter
λ_j^i =i-th incremental, j-th iterative analysis load factor
λ_1^1 =preset load increment factor
$\{\Delta\overline{U}\}$ =incremental displacement vector by unbalanced force vector
$\{\Delta\hat{U}\}$ =incremental displacement vector by total load vector

The sign of λ_1^1 at the right side in Eq. (7) indicates the load applying direction. If the sign is positive, the incremental load is applied in the same direction as that of the former incremental load. This sign is determined by the sign of *GSP*, the generalized stiffness parameter. If *GSP* has a positive sign, the sign of λ_1 has the same sign as that of λ_1^{i-1} which refers to the former incremental load factor. However, when GSP shows a negative value, the direction of loading is reversed by multiplying the λ_1 by −1.

2.4. Analysis procedure

For elastic buckling analysis of cable-stayed bridges

under construction, special analyses, initial shape analysis and construction stage analysis, should be performed. In fact, initial shape analysis can be included in the construction stage analysis if forward process analysis is used for construction stage analysis. If forward construction stage analysis is performed, initial shape analysis should be performed at every construction stage step. But, only one initial shape analysis is needed if backward process analysis is adopted for construction stage analysis. These analyses are described in following paragraphs.

2.4.1. Initial shape analysis for considering the dead load condition

In order to obtain the minimized deformed structural state under the dead load condition, optimum cable tensile forces should be decided using a rational initial shape analysis method. In this study, the initial force method for the initial shape analysis is used for determining the optimum cable tensile forces and the structural state which shows the minimum deformation and bending moments under the dead load condition (Wang *et al*., 1993; Wang

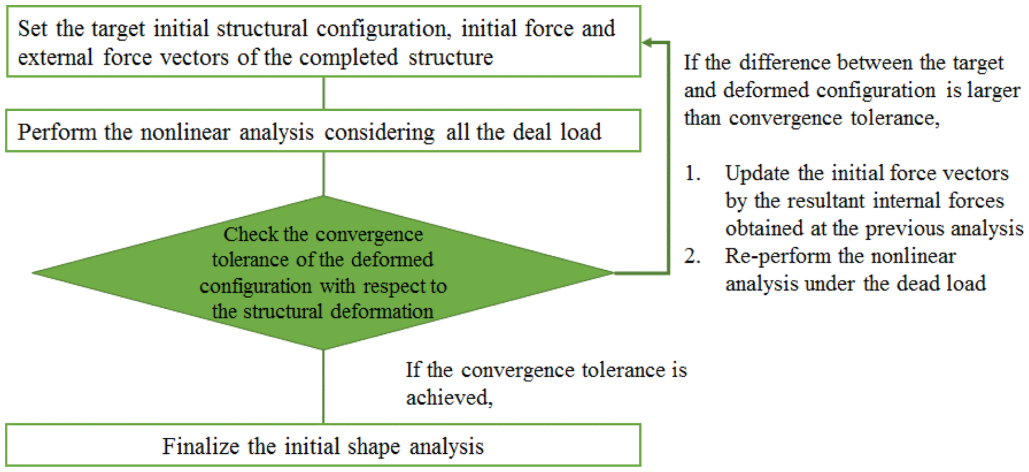

Figure 5. Procedure of initial shape analysis (initial force method).

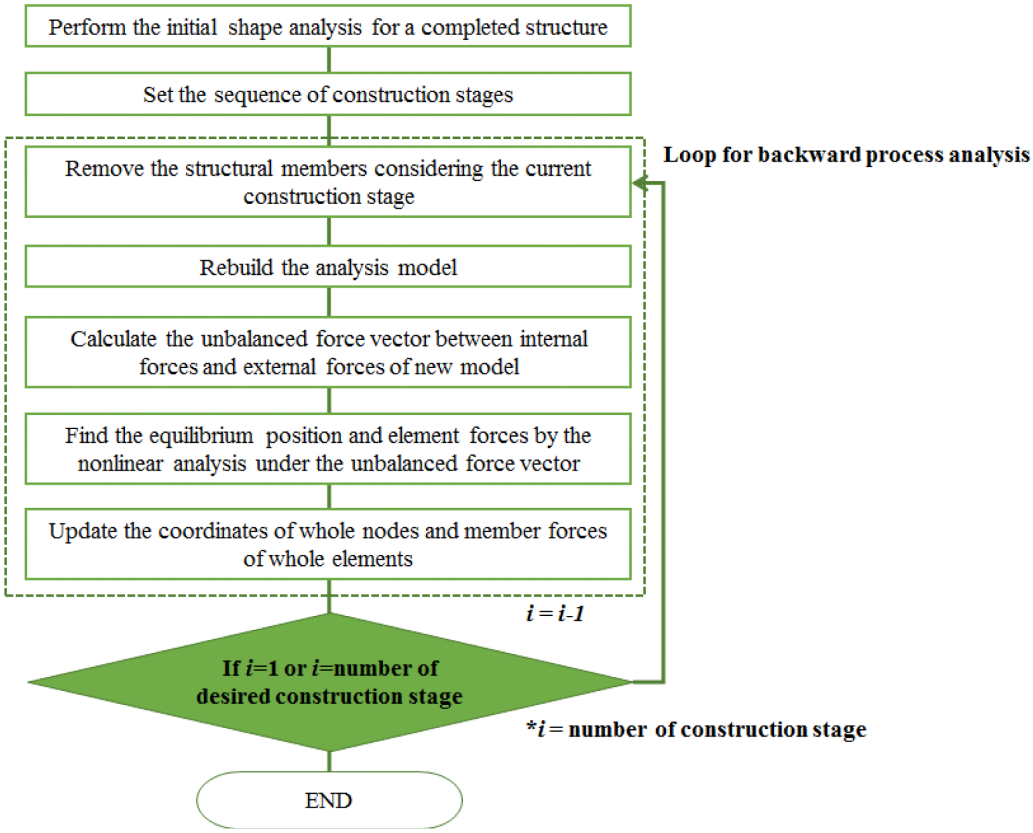

Figure 6. Backward process method for the construction stage analysis.

and Yang, 1993). This initial shape analysis is performed before the external load analysis and the construction stage analysis to obtain the target configuration with minimum deformation and bending moment of the girder. In this study, an initial force method is adopted for initial shape analysis. Figure 5 presents the analysis sequence of initial shape analysis using the initial force method.

2.4.2. Construction stage analysis

In general, cable-stayed bridges are constructed by being divided into detailed construction procedures. Construction stage analyses are performed to determine the structural state at various construction stages. There are two methods for construction stage analysis; the first is the forwarding process method, which traces the construction procedure following a positive direction; the second is the backward process method, which traces the construction procedure following the opposite direction (Wang *et al*., 2004). In this study, the characteristics of structural stability under construction of the erection of the key segment are focused on. To rationally consider the structural state under construction, construction stage analysis is performed before external load analysis. For efficient analytical study, the backward process method is adopted for construction stage analysis, because the last construction stage is the main focus of this research. Figure 6 shows the procedure of the backward process method.

2.4.3. Analysis strategy of elastic buckling analysis for cable-stayed bridges

Figure 7 presents the proposed elastic buckling analysis scheme for cable-stayed bridges under construction. Because the backward process analysis is used as the construction stage analysis, the initial shape analysis for the whole structure is performed first to find the structural state under dead load condition. In this step of the analysis, only the dead load is considered. Then, backward process analysis is performed to determine the structural state of the structure under construction, and finally the external force analysis is performed to analyze elastic buckling of cable-stayed bridges. All three analyses are performed based on the theory of nonlinear finite element analysis.

3. Numerical Validation

In this section, several analytical examples are introduced for verifying the developed analysis algorithm and method used in this study. Firstly, geometric nonlinear analyses using a nonlinear frame element and nonlinear equivalent truss element are described for verifying the nonlinear

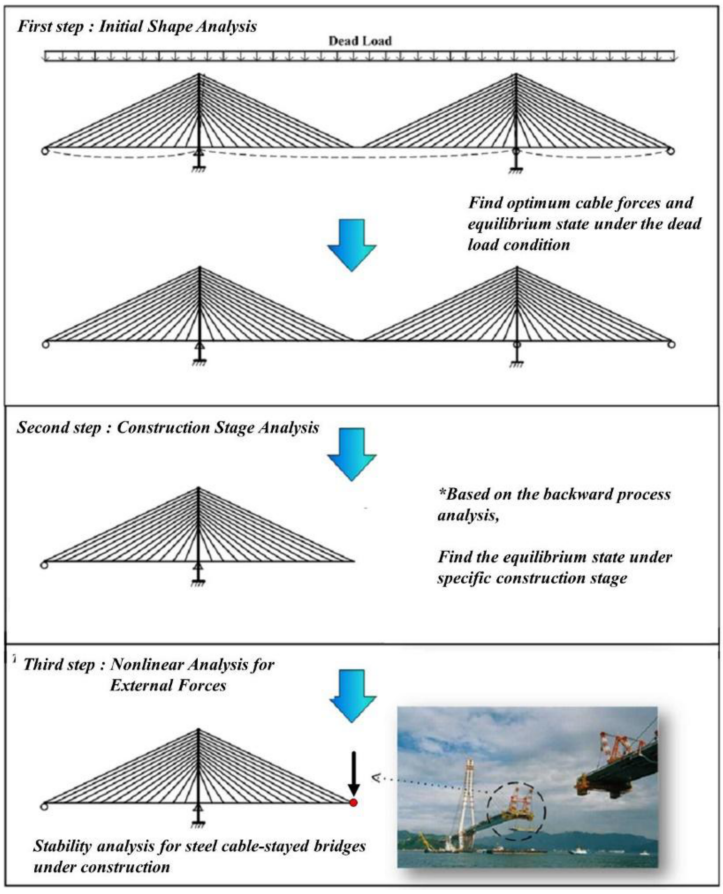

Figure 7. Proposed analysis strategy of elastic buckling analysis for cable-stayed bridges under construction.

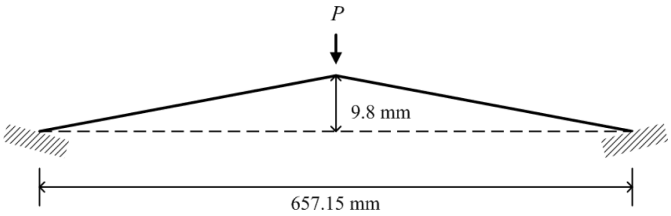

Figure 8. Williams' toggle frame.

elements and numerical solving scheme. Subsequently, the construction stage analysis is verified using the simple analytical model used in the former researches.

3.1. Nonlinear analysis for Williams' toggle frame which shows snap-through buckling

In order to verify the nonlinear frame element and numerical solving scheme, geometric nonlinear analysis is performed for the toggle frame shown in Fig. 8. As shown in the figure, a concentrated load is applied at the center of the structure. It is well known that snap-through buckling occurs due to the concentrated load being applied to the center of the structure. In this section, whether the developed program can trace the snap-through type buckling problem is verified.

For modeling this structure, 20 nonlinear frame elements are used. The geometric and material properties are shown in Table 1.

Figure 9 exhibits the load-displacement curves obtained by this developed program and ABAQUS V6.9, respectively. As shown this graph, the exact snap-through response is obtained by this developed program. As mentioned before, the generalized displacement control method is used in this study as the numerical scheme for solving complex nonlinear response. According to the comparison of results shown in Fig. 9, it can be concluded that complex nonlinear response can be traced by this program.

Table 1. Geometric and material properties of this example model

Elastic modulus	71,016 MPa (1.03×10^7 psi)
Section area	118.064 mm^2 (0.183 $in.^2$)
2nd moment of inertia	374.77 mm^4 (9.00×10^{-4} $in.^4$)

3.2. Nonlinear analysis for the cantilever beam supported by pre-stressed cable

In this section, the result of nonlinear analysis for the cantilever beam supported by the cable is introduced to verify nonlinear analysis using the nonlinear equivalent cable element and the nonlinear frame element. For modeling this structure, 10 nonlinear frame elements and 1 nonlinear equivalent truss element are used. As shown in Fig. 10, the distributed load applied to the cantilever beam is 98.1 kN/m and the pre tensile force applied to the cable member is 1,068 kN. The geometric and material properties of this model are shown in Table 2.

Figure 11 presents the vertical and rotational displacement obtained by nonlinear analysis using this developed program. These displacement components are compared with the former research results (Yun and Lee, 2001) obtained by nonlinear analysis using the elastic catenary cable

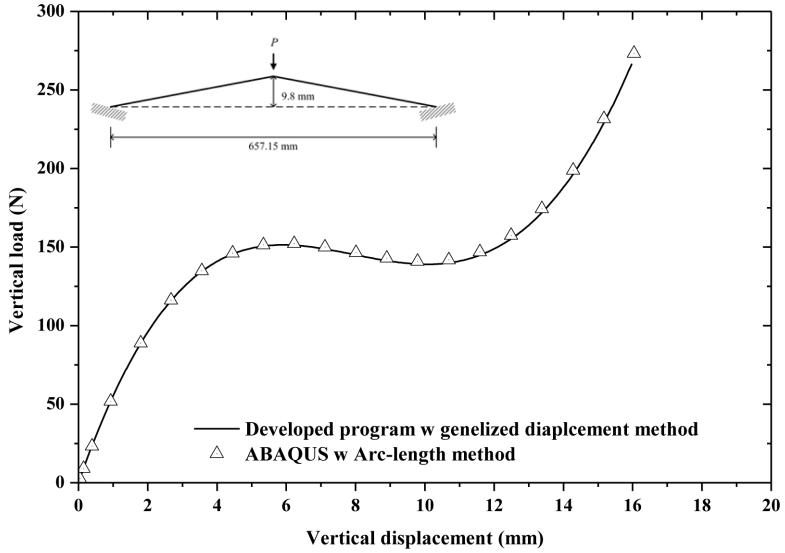

Figure 9. Load-displacement curve at the center of the structure.

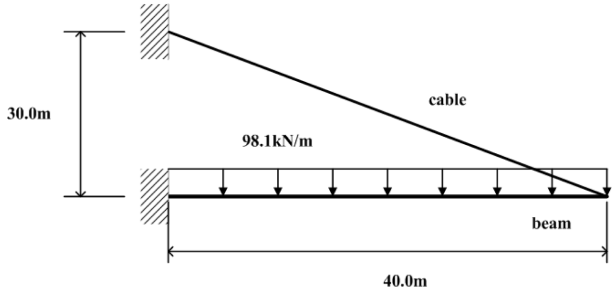

Figure 10. Cantilever beam supported by cable member

element. It is well known that analysis using the elastic catenary cable element can give analytical results that are the closest to the exact solution for cable members. However, it is also known that if the elastic catenary cable element is used for modeling the cable member, many calculations need to be made numerous times. As shown in Fig. 11, the analytical results are almost the same as the former results obtained by analysis using the elastic catenary cable element. This similarity occurs because an exact shape function is used in order to derive the equivalent elastic modulus for considering the cable sag effect. From this comparison, it can be concluded that rational analytical results can be obtained by nonlinear analysis using this nonlinear equivalent truss element for modeling cable members.

Table 2. Geometric and material properties of the structure

	Beam	Cable
Elastic modulus (kN/m^2)	2.1×10^8	2.1×10^8
Section area (m^2)	2.0	0.03
2nd moment of inertia(m^4)	0.04167	-
Weight per unit volume	77 (Not considered)	77

3.3. Construction stage analysis via backward process analysis

This section introduces a numerical example for verification of the construction stage analysis in this study. The following 2-dimensional cable-stayed bridge with 20 stayed cables is used for the analysis using the developed program. For verification, initial shape analysis and backward process analysis are performed and analyses results are compared with the results presented by former research of construction stage analysis, using forward process analysis (GS E&C, 2003) for verification of rationality of the developed program.

Figure 13 represents the bending moment distribution of girder and mast after the initial shape analysis. As shown in that figure, a uniform bending moment distribution is obtained by initial shape analysis using the developed program in this study.

As shown in Table 4, maximum (positive) and minimum (negative) bending moments in this study, as well as the maximum displacements, are smaller than the values obtained in the former research. The differences in internal forces and displacements are originated by the differences of the applied initial shape analysis methodologies with convergence tolerance about deflection under the dead

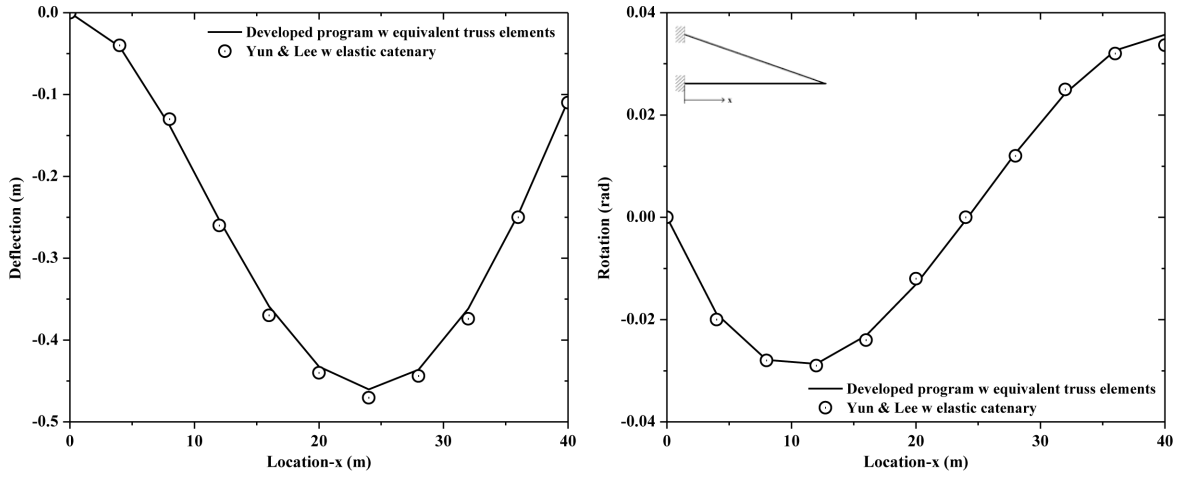

(a) Vertical displacements (b) Rotational displacements

Figure 11. Displacements of the cantilever beam.

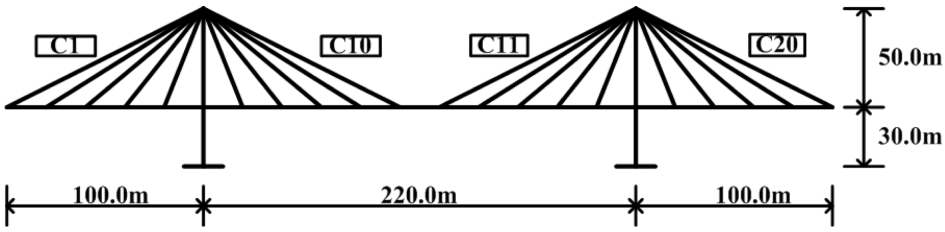

Figure 12. Example model.

Table 3. Material and geometric properties of main members

Member		A (m^2)	I (m^4)	γ (kN/m^3)	E (kN/m^2)
Girder		0.80	1.0	120.0	2.1×10^8
Mast	Upper	5.0	10.0	78.0	2.1×10^8
	Lower	10.0	20.0	78.0	2.1×10^8
Cable		0.006 ~0.011	-	78.0	2.0×10^8

load condition. With more strict convergence tolerance about deflection, applied analysis algorithm found more optimum initial condition. The comparison results indicates that the applied analysis algorithm in this study can be used for obtaining the optimum target structural state under the dead load condition.

Figure 14 exhibits the deformed shape after construction stage analysis using the developed program. As shown in Fig. 14, the tip of the right end in the under construction model has risen due to tensile forces of cables which support the girder of the middle span. After backward process analysis, the upward displacement of the tip of the right end in the model is 0.10 m, while the horizontal displacement of the top of the mast is 0.025 m.

Figure 15 shows the distribution of bending moments after the construction stage analysis. Due to redistributed cable tensile forces, upward displacements occur at the girder of the center span. So, positive bending moments at the girder nearby joint between the girder and the mast are observed, because of these upward bending deformations of the center span.

Table 5 compares the bending moments and displacements of this study with those of former research. The maximum positive bending moment by this study is larger than the value by former research, while the maximum negative bending moment by this study is smaller than the value by former research. There are some differences in performing the construction stage analysis, such as the method of construction stage analysis (forward process analysis vs backward process analysis), used elements,

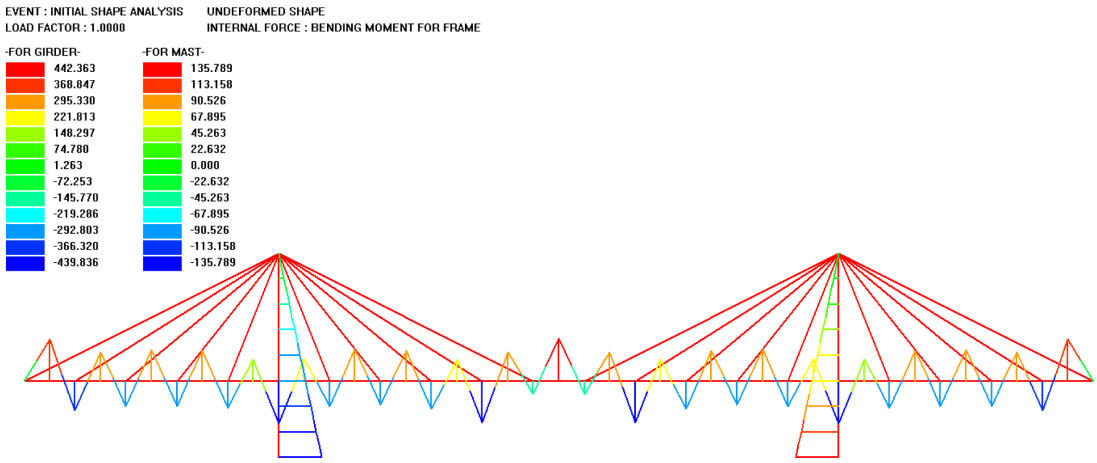

Figure 13. Bending moment distribution after the initial shape analysis (Maximum/Minimum bending moment at the girder: 442.36/–439.84 tonfm).

Table 4. Comparison of the bending moments and displacements after initial shape analysis

Bending moments and displacements		(GS E&C)	This study	Diff. (%)
Bending moments (kN·m)	Maximum Positive	4,636.4	4,335.13	-6.50
	Minimum Negative	-4,452.14	-4310.43	-3.18
Displacement (m)	Vertical displacement at the center of the middle span	0.028	0.0064	-77.14
	Horizontal displacement at the top of the mast	-0.012	-0.00084	-93.00

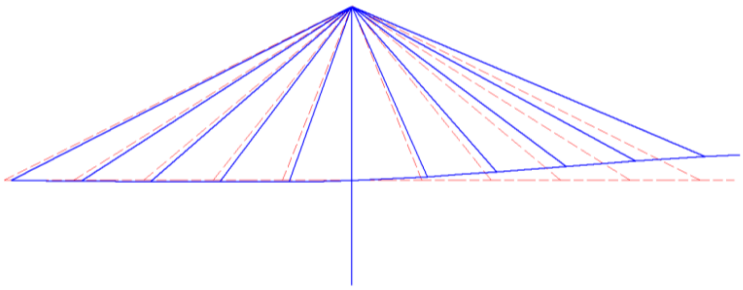

Figure 14. Deformed shape after construction stage analysis (Scale factor: 50.0)

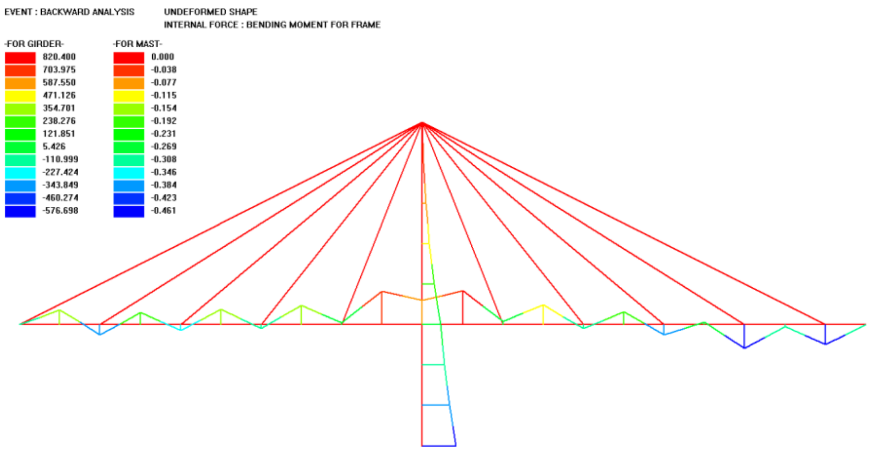

Figure 15. Bending moment distribution after the construction stage analysis (Maximum/Minimum bending moment at the girder: 828.4/-579.7 tonfm).

Table 5. Comparison of the bending moments and displacements after construction stage analysis

Bending moments and displacements		(GS E&C)	This study	Diff. (%)
Bending moments (kN·m)	Positive	7,331.38	8,039.91	9.66
	Negative	-6,434.68	-5,651.64	-12.17
Displacement (m)	Vertical displacement at the center of the middle span	0.09	0.10	11.11
	Horizontal displacement at the top of the mast	-0.029	-0.025	-13.79

boundary conditions, and control options for nonlinear analysis. Although there are some differences in the bending moments, results after the construction stage analysis are very similar, such as the deformation (configuration) and bending moment diagrams. So, it can be proven that this developed program can be used to investigate the nonlinear behavior of cable-stayed bridges under construction, as well as completed structures.

4. Structural Stability of Cable-stayed Bridges under Construction Stage

4.1. Analysis model

In this chapter, a study of structural stability of cable-stayed bridges under construction is described. To analyze elastic buckling characteristics of the structure, the developed program referred to previous chapters is used. With rational evidences, governing buckling modes are classified into two categories in this chapter. Further, the effect of cable-arrangement type and girder-mast stiffness ratio on structural stability is studied and presented.

Figures 16 and 17 show analysis models considered in this study. These show two different cable-arrangement types that are considered to investigate the effect on structural stability. As mentioned before, initial shape analysis for the whole structure (which means the completed structure) is performed first, and then construction stage analysis is performed to trace the equilibrium state of the construction stage model. After that, nonlinear analysis for the stability analysis under external load condition is performed. Figure 18 shows the section of the girder. The section of the mast is considered as a box section, of various sectional sizes to investigate the effect of mast stiffness. It is assumed that there are sufficient stiffeners to prevent local buckling in the section of the girder and mast. Finally, a circular section is considered as the

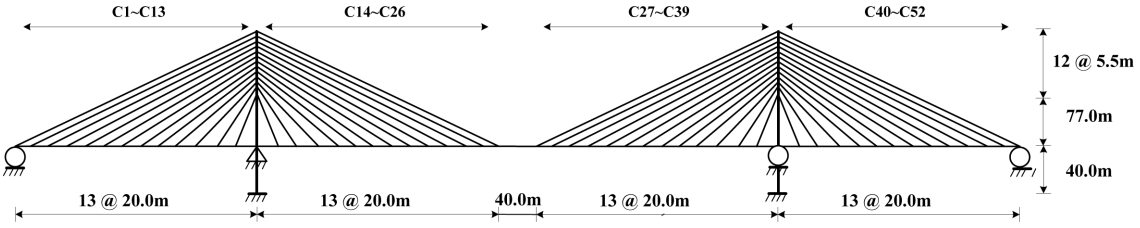

(a) Fan type model

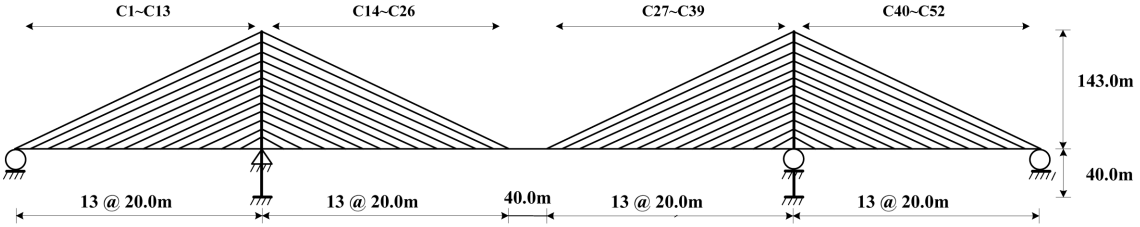

(b) Harp type model

Figure 16. Completed analysis model.

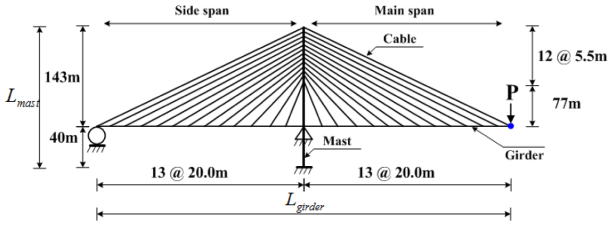

(a) Fan type model

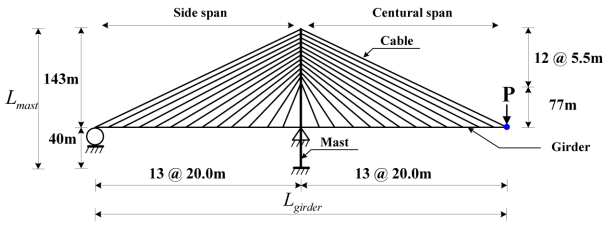

(b) Harp type model

Figure 17. Analytical model under Construction Stage.

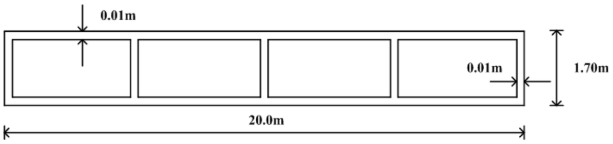

Figure 18. Section of the girder.

Table 6. Material and geometric properties of main members

	Girder	Mast	Cable
E (kN/m^2)	2.1×10^8	2.1×10^8	2.1×10^8
A (m^2)	0.484	0.214~1.006	0.01~0.12
I (m^4)	0.305	0.214~10.719	-
ρ (kN/m^3)	157.74	78.0	78.0

Table 7. Considered girder-mast stiffness ratio

	Fan type	Harp type
$\frac{E_m I_m / L_m}{E_g I_g / L_g}$	2.00~50.00	2.00~50.00

section of the cable and various areas are considered to investigate the effect on the structural stability. Table 6 represents the material and geometric properties of girder, mast, and cables. In this study, girder-mast stiffness ratio is considered as the main parameter, which mainly affects the characteristics of structural stability. After extensive parametric study, typical buckling modes are classified into two types, and effects of the girder-mast stiffness ratio and cable area on the structural stability are investigated. Table 7 shows the range of girder-mast stiffness ratio considered in this study.

where,

E_m : Elastic modulus of a mast
E_g : Elastic modulus of a girder
I_m : 2nd Moment of inertia of a mast
I_g : 2nd Moment of inertia of a girder
L_m : Length (Height) of the mast
L_g : Length of the girder

Figure 19 presents the loading/boundary condition and analysis scheme. As shown this figure, the analytical model which has been performed backward process analysis is subjected to the concentrated load that reflects the weight of derrick crane and a key segment of the girder. Thus, buckling analysis is performed by three-step analysis, namely initial shape analysis, backward process analysis, and external load analysis.

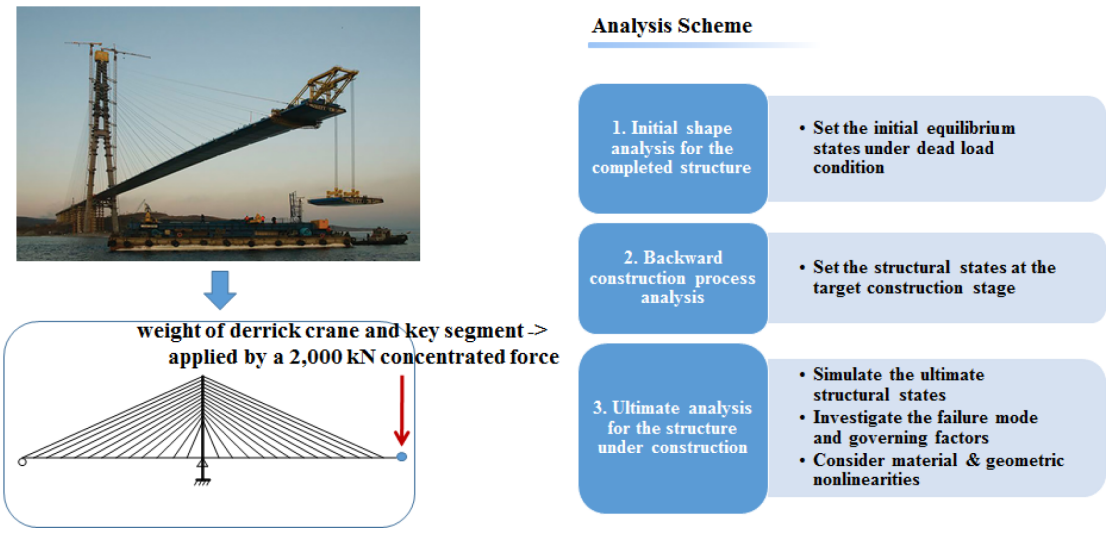

Figure 19. Loading/Boundary condition and Analysis scheme.

4.2. Elastic buckling mode 1: Girder-mast interactive buckling mode

When external load, which reflects the dead load of the derrick crane and a key segment, is applied to the tip of the center span of the analysis model as a concentrated force, the center span shows vertical deflection, and the mast shows horizontal movement. With this deformation, the tensile forces of stay cables also change. Thus, compressive forces applied to the girder and mast change as the external force increases. Because of the continuous increase of the external force, the compressive forces induced by stay cables also continuously increase. Finally, the structure reaches the critical state, with global buckling behavior. In this behavior, the beam-column effect of the girder and mast is very interesting. When the external force is applied to the tip of the center span, girder and mast show flexural deformation because of the vertically applied force. By the way, the girder and mast are already subject to compressive force by the stay cables which initially have tensile forces. As the external force increases, the flexural deformation of girder and mast increases. The tensile forces of the stay cables also increase, in order to resist deformation of the structure. Thus, the flexural deformation of the girder and mast is amplified because of increasing compressive forces. Consequently, the girder and mast may buckle when vertical forces are applied to the girder, due to the beam-column effect being amplified by the interaction between flexural behavior and compressive force.

The first governing buckling mode introduced in this study is the girder-mast interactive buckling mode. When the mast doesn't have sufficient flexural stiffness, it also buckles as well as the girder, due to the increased compressive forces induced by the stay cables. Figure 20 shows the deformed shapes of the interactive buckling mode. In this buckling mode, girder and mast buckle together, because of the applied compressive forces induced by the stay cables. As external force is applied to the tip of the center span girder, the center span deflects and flexural deformation occurs. This deformation leads the deformation of the mast by stay cables. So, the mast shows horizontal movement and flexural deformation, while the girder shows flexural deformation. Increase of the external force makes for more bending deformation of girder and mast with the increase of tensile forces in the cables. Therefore, the beam-column effect and behavior are induced by the flexural behavior and compressive forces. As shown in Fig. 20, girder and mast buckle together with flexural bending deformation. Figures 21 and 22 show the buckling procedure obtained by incremental analysis.

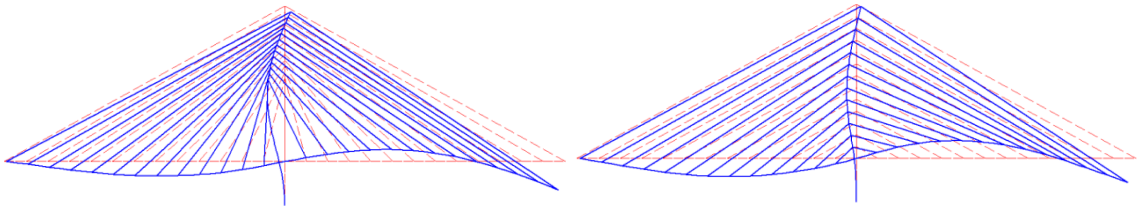

(a) Fan type model (b) Harp type model

Figure 20. Girder-mast interactive buckling mode (girder-mast stiffness ratio=2.0)

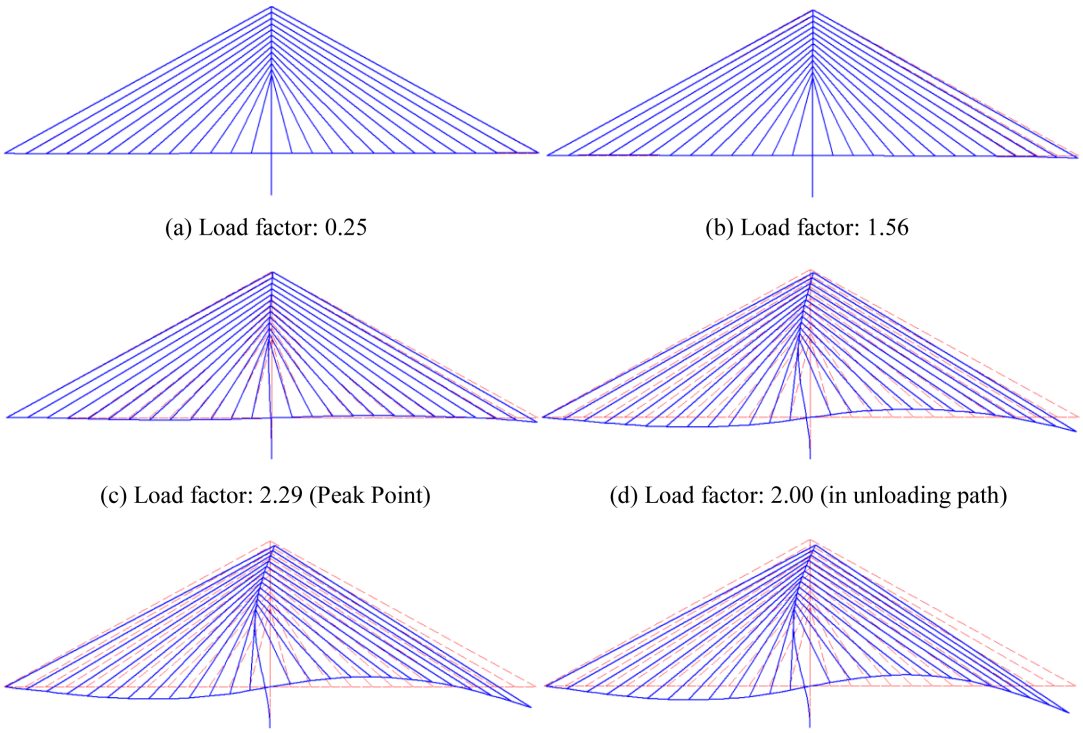

(a) Load factor: 0.25 (b) Load factor: 1.56

(c) Load factor: 2.29 (Peak Point) (d) Load factor: 2.00 (in unloading path)

(e) Load factor: 1.80 (in unloading path) (f) Load factor: 1.64 (in unloading path)

Figure 21. Interactive buckling procedure of fan type model (girder-mast stiffness ratio: 2.0).

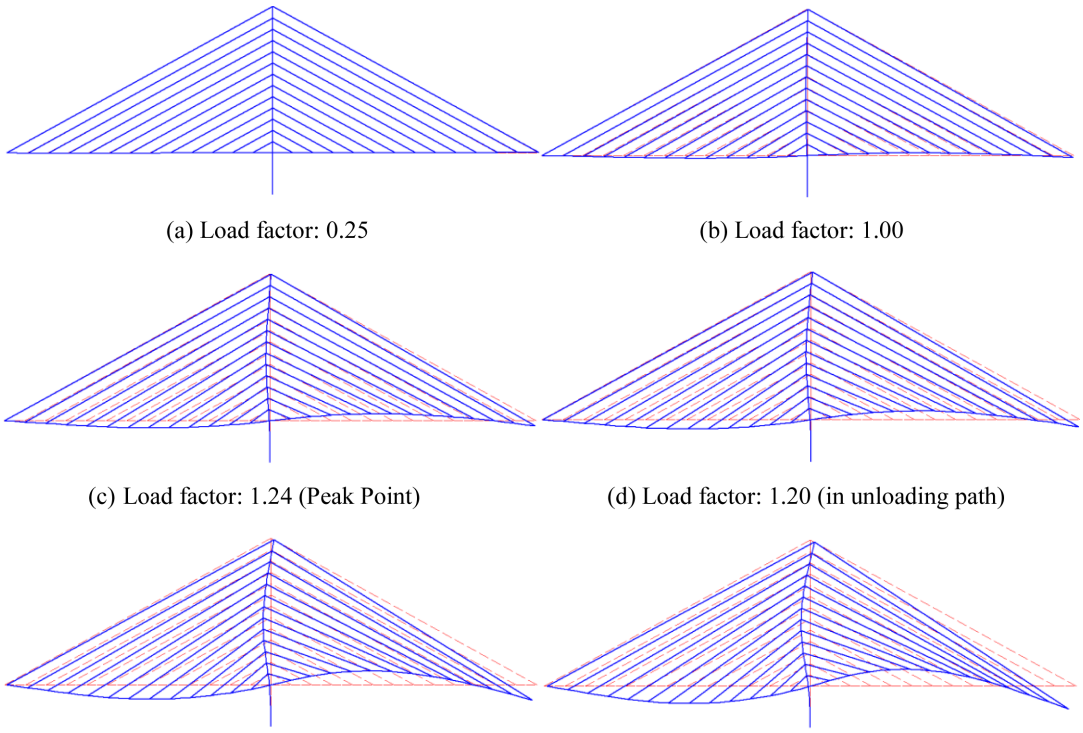

(a) Load factor: 0.25 (b) Load factor: 1.00

(c) Load factor: 1.24 (Peak Point) (d) Load factor: 1.20 (in unloading path)

(e) Load factor: 1.00 (in unloading path) (f) Load factor: 0.84 (in unloading path)

Figure 22. Interactive buckling procedure of harp type model (girder-mast stiffness ratio: 2.0).

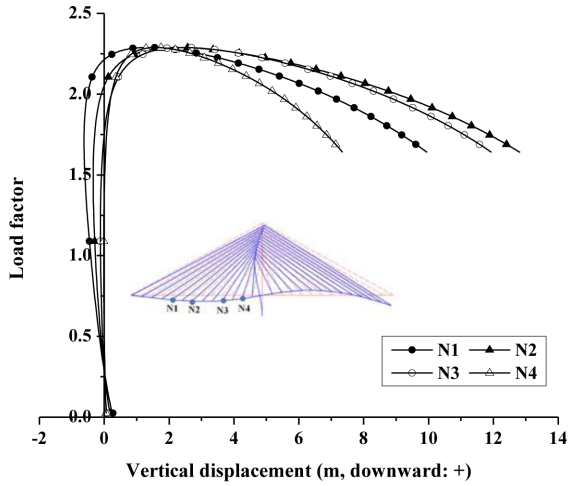

(a) Points at the left side spangirder

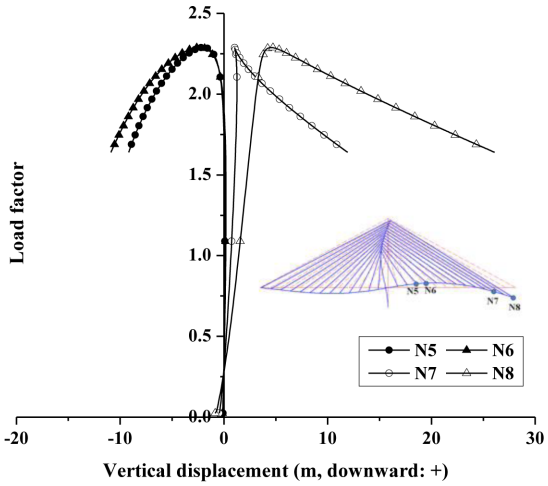

(b) Points at the center span girder

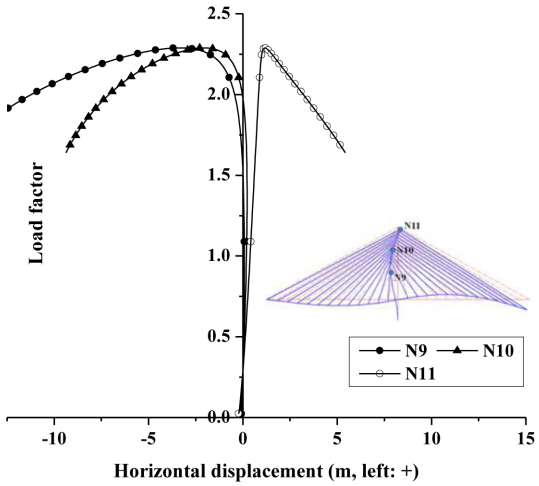

(c) Points at the mast

Figure 23. Load-displacement curves of fan type model, girder-mast stiffness ratio: 2.0).

Figures 23 and 24 show the load-displacement curves of each model, which demonstrate the interactive buckling mode. As the external load increases, upward and downward displacements also increase. As shown in Figs. 23(b) and 24(b), upward deformation occurs at the center span near a mast. As mentioned before, this is caused by the amplified beam-column effect, although the external load is applied at the tip of the center span with a downward direction. After the external load factor reaches the critical point, each displacement increases with an external load decrease. In other words, the structure becomes unstable, and large deformation occurs due to the girder-mast buckling.

As shown in these figures, there are clear critical points. After the external load factor reaches the critical load factor, the load factor starts to decrease. While the external load decreases, displacements and deformation of the structure increase. These behaviors validate the structural instability. Because main members of the structure buckle, structural deformation increases continuously, although the external load decreases.

As shown in Figs. 23(a) and 23(b), and 24(a) and 24(b), some points show a directional change in displacement. This is induced by the beam-column effect. As the beam-column effect is amplified with increasing compressive forces, flexural deformations of the girder and mast increase gradually. So, the directional change of the displacement occurs as the external load increases.

4.3. Elastic buckling mode 2: Girder buckling mode

The second buckling mode introduced in this study is a girder buckling mode. It can be supposed that if the mast has sufficient stiffness, only the girder may buckle. According to the analysis results of this research, when the mast has sufficient stiffness, only the girder of center span buckles. Figure 25 shows the deformed shapes of girder buckling mode.

As shown in Fig. 25, the girder of the center span buckles showing negative bending deformation. This deformation

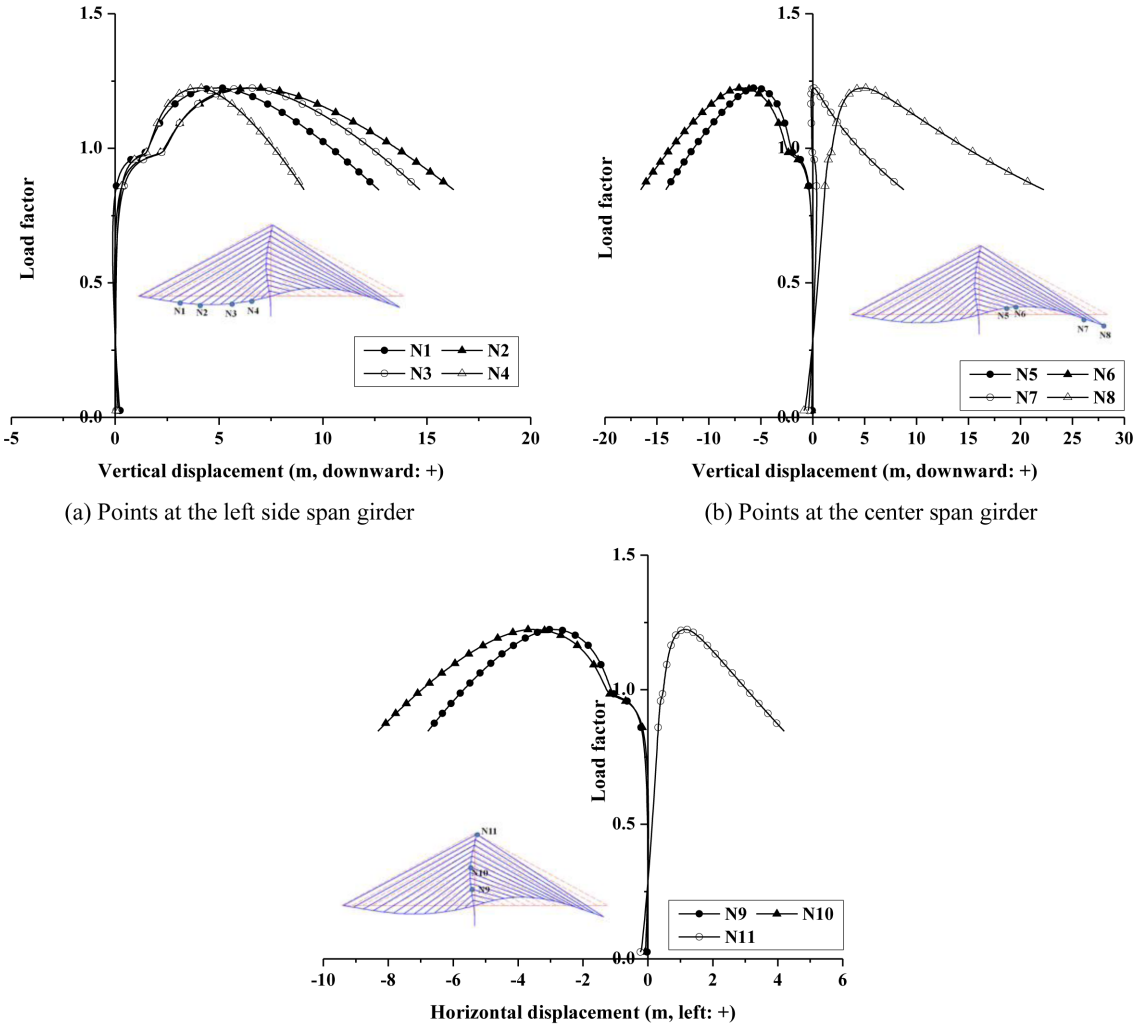

(a) Points at the left side span girder

(b) Points at the center span girder

(c) Points at the mast

Figure 24. Load-displacement curves of harp type model, girder-mast stiffness ratio: 2.0).

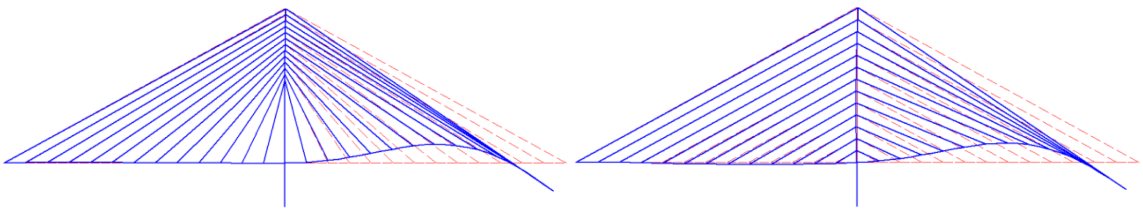

(a) Fan type model

(b) Harp type model

Figure 25. Girder buckling mode (girder-mast stiffness ratio=30.0)

is caused by the amplified beam-column effect due to the increasing compressive forces and bending behavior of the girder. Because the mast has sufficient stiffness, there is no significant horizontal movement of the mast, and the girder of the center span buckles only when the vertical force acts on the tip of the center span. Figures 26 and 27 show the buckling procedure obtained by incremental analysis.

Early in the process, the left span and center span girder show slight flexural deformation, while the mast doesn't show significant horizontal movement or flexural deformation. Each flexural deformation of the side span and the center span occurs by different reason. Actually, flexural deformation of the center span is caused by the vertically applied force, while flexural deformation of the side span is caused by the lifting effect due to slight horizontal movement of the mast. When vertical force is applied to the tip of the center span, vertical deflection occurs at the center span.

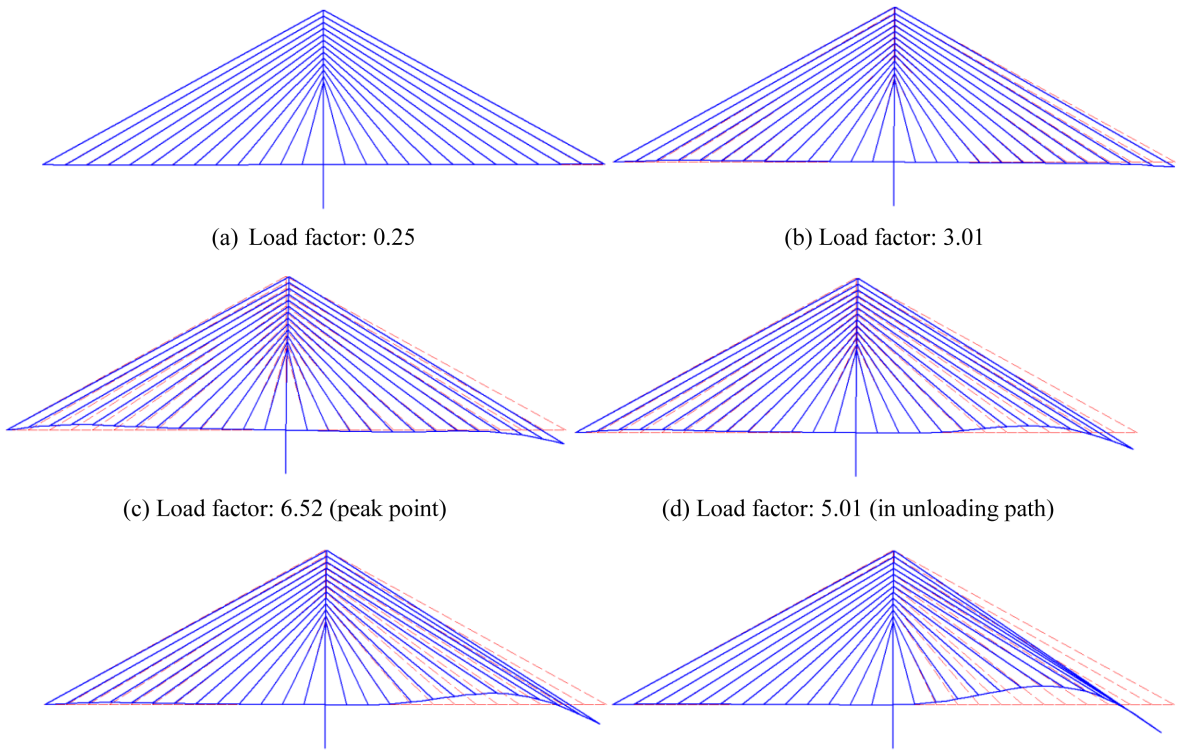

(a) Load factor: 0.25 (b) Load factor: 3.01

(c) Load factor: 6.52 (peak point) (d) Load factor: 5.01 (in unloading path)

(e) Load factor: 4.02 (in unloading path) (f) Load factor: 1.64 (in unloading path)

Figure 26. Girder buckling procedure of fan type model (girder-mast stiffness ratio: 30.0).

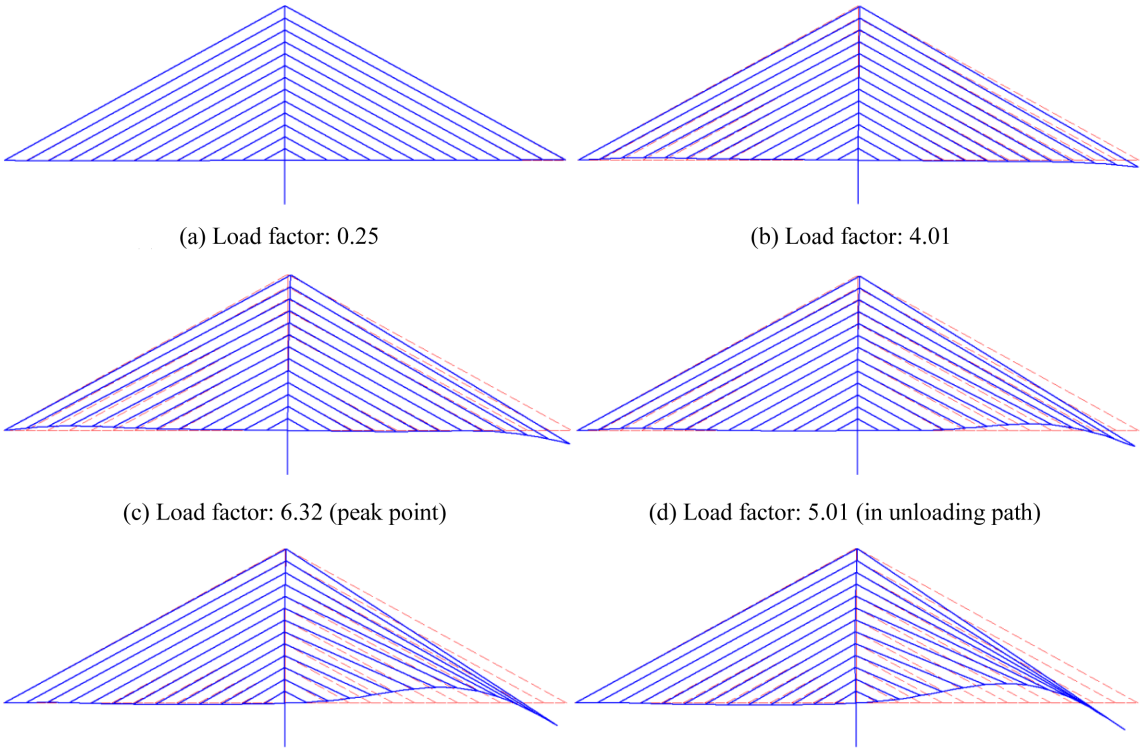

(a) Load factor: 0.25 (b) Load factor: 4.01

(c) Load factor: 6.32 (peak point) (d) Load factor: 5.01 (in unloading path)

(e) Load factor: 3.01 (in unloading path) (f) Load factor: 2.28 (in unloading path)

Figure 27. Girder buckling procedure of harp type model (girder-mast stiffness ratio: 30.0).

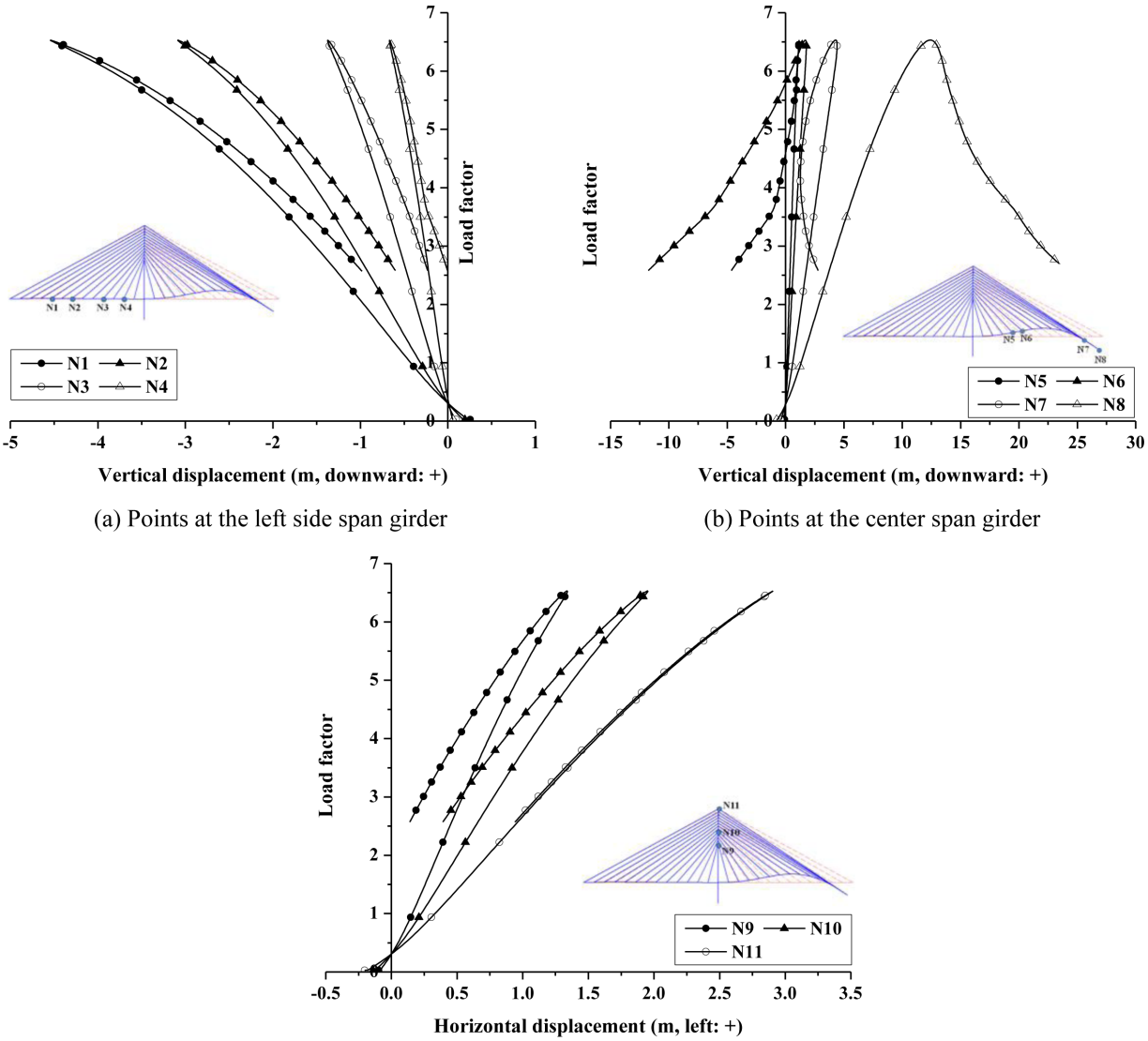

(a) Points at the left side span girder

(b) Points at the center span girder

(c) Points at the mast

Figure 28. Load-displacement curves of fan type model, girder-mast stiffness ratio: 30.0)

This vertical deflection of the center span leads to the horizontal movement and flexural deformation of the mast, because of girder-mast-cable interaction. As the mast suffers horizontal movement, the side span is lifted by the stay cables. So, there is flexural deformation induced by different causes at both spans.

After the critical state, i.e. the load factor reaches the critical point, the load factor starts to decrease. In the load decrease path, flexural deformation of the center span is amplified, while flexural deformation of the left side span and horizontal movement of the mast are recovered. As the beam-column effect of the center span is amplified, upward deformation occurs at the center span near the mast, while the tip of the center span moves continuously downward. This deformation lasts, although the external load decreases. It validates the thesis that the center span buckles due to an amplified beam-column effect. Although the external force decreases, downward deformation of the tip increases continuously, thus tensile force of the exterior cable increases also. Of course, other cables that support the center span may lose tensile force, because of upward deformation of the center span. But, the tensile force of the exterior cable which has the largest tensile force increases continuously, because of sustained downward deflection of the tip of the center span. So, the girder of the center span is subject to increasing compressive forces, and amplifies the beam-column effect. Finally, the girder of the center span buckles, while other main members recover the deformation when the external load decreases.

Figures 28 and 29 represent load-displacement curves of the fan type and harp type model, which show the girder buckling mode. As shown in these figures, the girder of the center span buckles with a negative bending deformation, and this deformation grows continuously

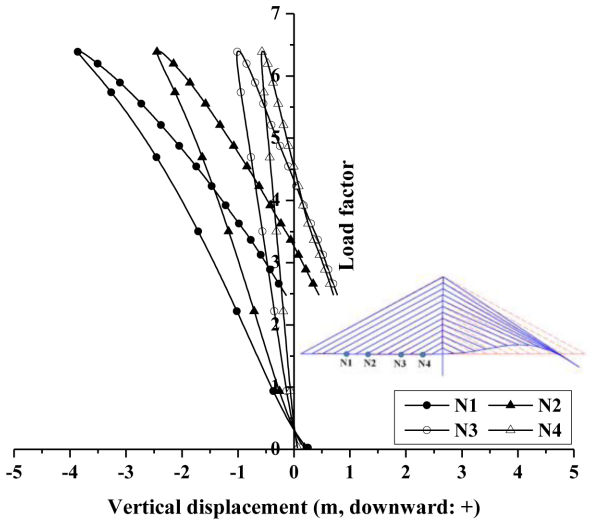

(a) Points at the left side span girder

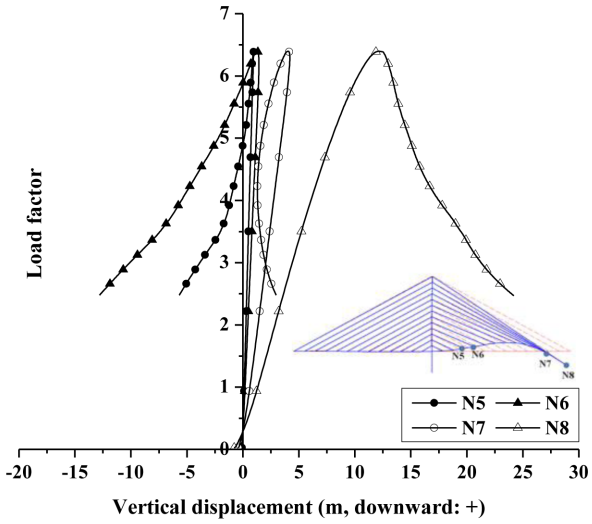

(b) Points at the center span girder

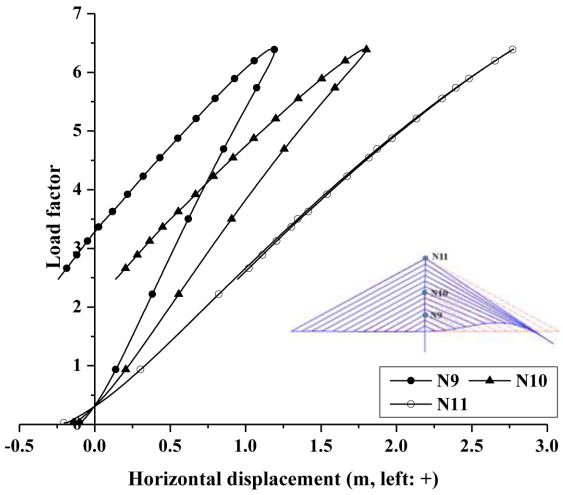

(c) Points at the mast

Figure 29. Load-displacement curves of harp type model, girder-mast stiffness ratio: 30.0)

after the load factor reaches the critical point and the load decreases. As mentioned previously, the side span and mast recover the deformation as the external force decreases. Because the structural stiffness changes suffering large deformation, deformation of the girder and mast show an unloading path, which is not same as the loading path. While side span and mast recover their deformation, the girder of the center span buckles continuously, because of an amplified beam-column effect. This buckling mode can be classified as the second buckling mode introduced in this study. This buckling mode may occur when the mast is designed with sufficient flexural stiffness.

4.4. Effect of girder-mast stiffness ratio

In this chapter, the effect of girder-mast stiffness ratio on the buckling mode is described. In order to study the effect, analysis models are designed with different sections of mast. The range of girder-mast stiffness ratio considered is 2.0 to 50.0. Figures 30 and 31 show governing buckling modes with respect to girder-mast stiffness ratio. As shown in these figures, the buckling mode changes from girder-mast interactive buckling to girder buckling as the girder-mast stiffness ratio increases. In other words, the girder buckling mode governs the global buckling of cable-stayed bridges under construction, provided the mast is designed with sufficient flexural stiffness. It can be said that the more ideal buckling mode is the girder buckling mode because mast buckling means entire loss of support ability for the structure. As shown by the analysis results, critical load factors of the girder-mast interactive buckling mode are lower than critical load factors of the girder buckling mode. Therefore, the mast should be designed by considering the minimum required flexural stiffness in order to prevent girder-mast interactive buckling.

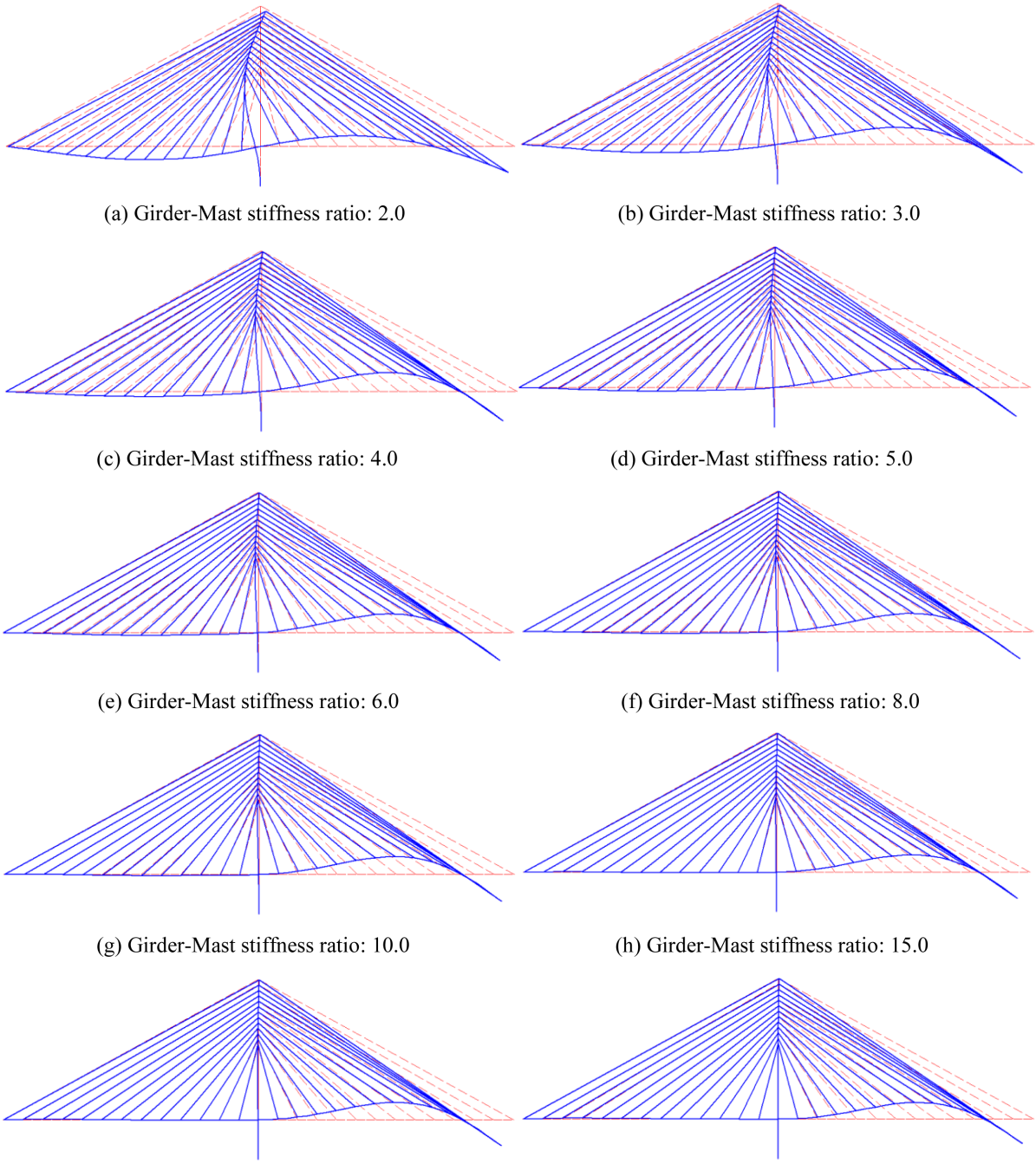

(a) Girder-Mast stiffness ratio: 2.0 (b) Girder-Mast stiffness ratio: 3.0

(c) Girder-Mast stiffness ratio: 4.0 (d) Girder-Mast stiffness ratio: 5.0

(e) Girder-Mast stiffness ratio: 6.0 (f) Girder-Mast stiffness ratio: 8.0

(g) Girder-Mast stiffness ratio: 10.0 (h) Girder-Mast stiffness ratio: 15.0

(i) Girder-Mast stiffness ratio: 20.0 (j) Girder-Mast stiffness ratio: 40.0

Figure 30. Buckling mode of fan type models with respect to girder-mast stiffness ratio.

Figure 32 shows the change of critical load factor as the girder-mast flexural stiffness changes. As shown by the figure, the critical load factor increases as the girder-mast stiffness ratio increases. But the critical load factor converges to a certain value as the girder-mast stiffness ratio increases more and more. According to the analysis results, the critical load factor shows significant increase, until the governing buckling mode changes to girder buckling mode. In order words, there was no significant increase of the critical load factor in girder buckling mode. When the mast has sufficient flexural stiffness, significant horizontal movement of the mast does not occur, although the tip of the center span suffers vertical deflection by applied vertical load. Also, the side span suffers relatively little lifting caused by horizontal movement of the mast. Therefore, only flexural stiffness of the girder affects the critical load factor, mainly when the girder buckling mode governs structural stability. In this study, the section of the girder

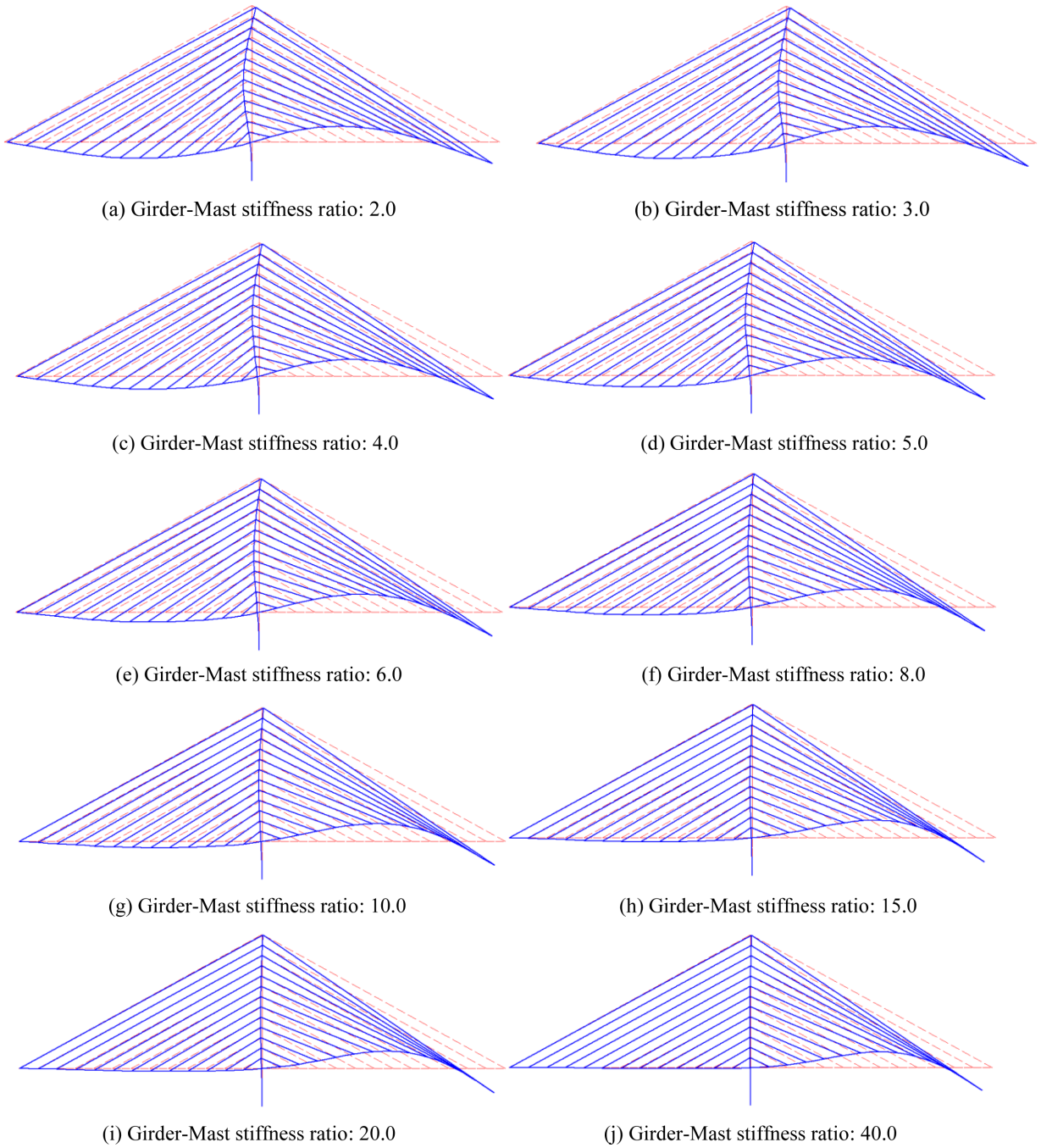

(a) Girder-Mast stiffness ratio: 2.0

(b) Girder-Mast stiffness ratio: 3.0

(c) Girder-Mast stiffness ratio: 4.0

(d) Girder-Mast stiffness ratio: 5.0

(e) Girder-Mast stiffness ratio: 6.0

(f) Girder-Mast stiffness ratio: 8.0

(g) Girder-Mast stiffness ratio: 10.0

(h) Girder-Mast stiffness ratio: 15.0

(i) Girder-Mast stiffness ratio: 20.0

(j) Girder-Mast stiffness ratio: 40.0

Figure 31. Buckling mode of fan type models with respect to girder-mast stiffness ratio.

is constant, while the section of the mast varies. Eventually, the critical load factor converges to a specific value, as sufficient flexural stiffness of the mast is considered.

There is another interesting point shown in the figure. In general, critical load factors of fan type models are larger than critical load factors of harp type models when these two models have the same girder-mast stiffness ratio. This is caused by the difference of horizontal angle of the cable-arrangement. It can be explained by the principle of force equilibrium. When the same vertical load is applied to the same point, the cable with the lower horizontal angle requires a larger tensile force than the cable with a higher horizontal angle. Therefore, the girder of the harp type model is subjected to larger compressive force than the girder of the fan type model under the same vertically applied loading condition. Moreover, the mast of the harp type model suffers a larger horizontal movement than the mast of the fan type model. Therefore, the critical load factors of fan type models are larger than the critical load factors of harp type models.

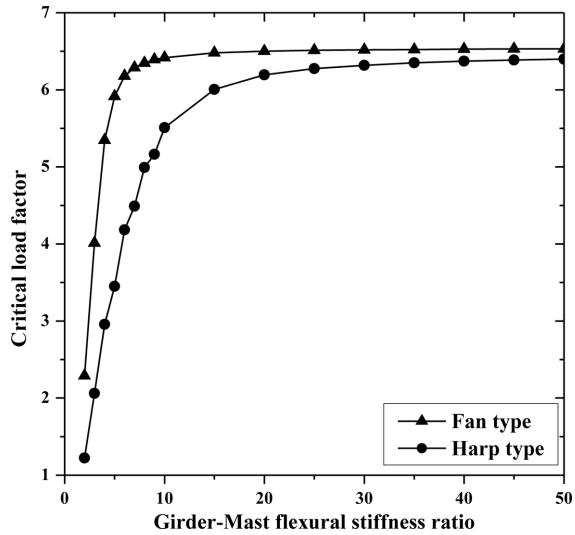

Figure 32. Girder-mast flexural stiffness ratio vs critical load factor

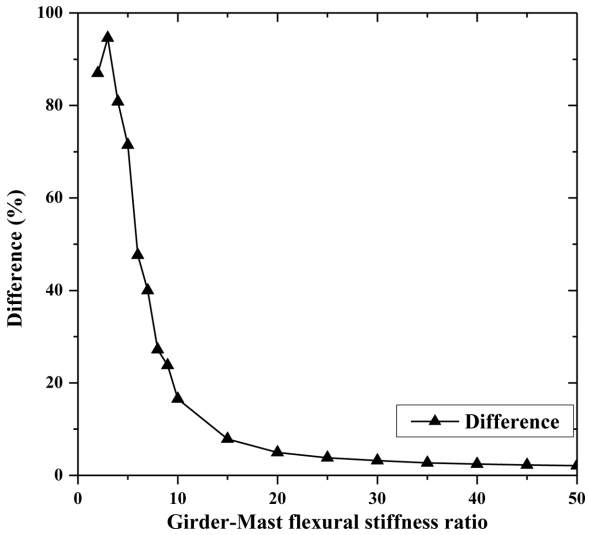

Figure 33. Change of difference of critical load factor.

By the way, the difference in critical load factors between the two models decreases as the girder-mast stiffness ratio increases. In order words, the governing buckling mode changes to the girder buckling mode.

Figure 33 shows the decrease of the difference of critical load factors between the two models. Difference percentages are calculated as follows:

(Critical load factor of the fan type model–Critical load factor of the harp type model)/Critical load factor of the harp type model×100 (%) (11)

As shown in Fig. 33, the difference also converges to a specific value. This can be explained with the change of cable tensile forces.

As shown in Fig. 34, cables that support the center span show force decreases, except for C15, C16 and C17, which are near the mast, and C25 and C26, which are near the tip of the span. This force decrease is caused by upward flexural deformation of the girder when the girder of center span buckles. As the relative distance between two nodes of the cable decreases, the tensile force of the cable decreases. As shown in the figure, tensile forces of cables C25 and C26 are extremely large, compared with other cables in the center span. This indicates that tensile forces of these two cables become the main source of the compressive forces applied to the center span. By the way, horizontal angles of C26 of the fan type model and harp type model are the same as each other. Also, horizontal angles of C25 of the fan type model and harp type model are very similar. Therefore, critical load factors of these two models become similar, because many cables loss their tensile forces due to buckling of the center span.

This can also be explained by Figs. 35 and 36, the external load-cable force curves of each model.

As shown in Figs. 35 and 36, C20~C24 in the center span show a force decrease as the external force increases. As mentioned previously, this is due to the girder buckling with upward deformation of the center span. In contrast, tensile forces of C25 and C26 increase until the external load factor reaches the peak point, due to continuous vertical deflection of the tip of the center span. Therefore, the girder of the center span is mainly subject to compressive force by the two exterior cables, C25 and C26. Horizontal angles of C26 in fan type model and harp type model are exactly the same as each other; and horizontal angles of C25 in both models are almost the same as each other; therefore, critical load factors of both two models in girder bucking mode are almost the same as each other, because of these characteristics of this buckling behavior.

4.5. Effect of the cable area

In this chapter, the effect of the cable area on the structural stability of cable-stayed bridges under construction is described. For this study, analysis models were classified into two categories of governing buckling mode, girder-mast interactive buckling mode and girder buckling mode. So the effects of each buckling mode are described separately. For investigating the effect on the girder-mast interactive buckling mode, analytical models with a girder-mast stiffness ratio of 2.0 are used. For investigating the effect on the girder buckling mode, analytical models which have a girder-mast stiffness ratio of 50.0 are used. Figure 37 shows the change of critical load factors with respect to the change of cable area.

As shown in Fig. 37, in girder-mast interactive buckling mode, the critical load factor decreases as the cable area increases. In general, it might be thought that increase of the cable area will lead to an increase in structural stability, because the cable is the intermediate supporting system of cable-stayed bridges. If the cable area increases, the elastic stiffness of the cable also increases. But the weight of the cable also increases, and it can lead to an

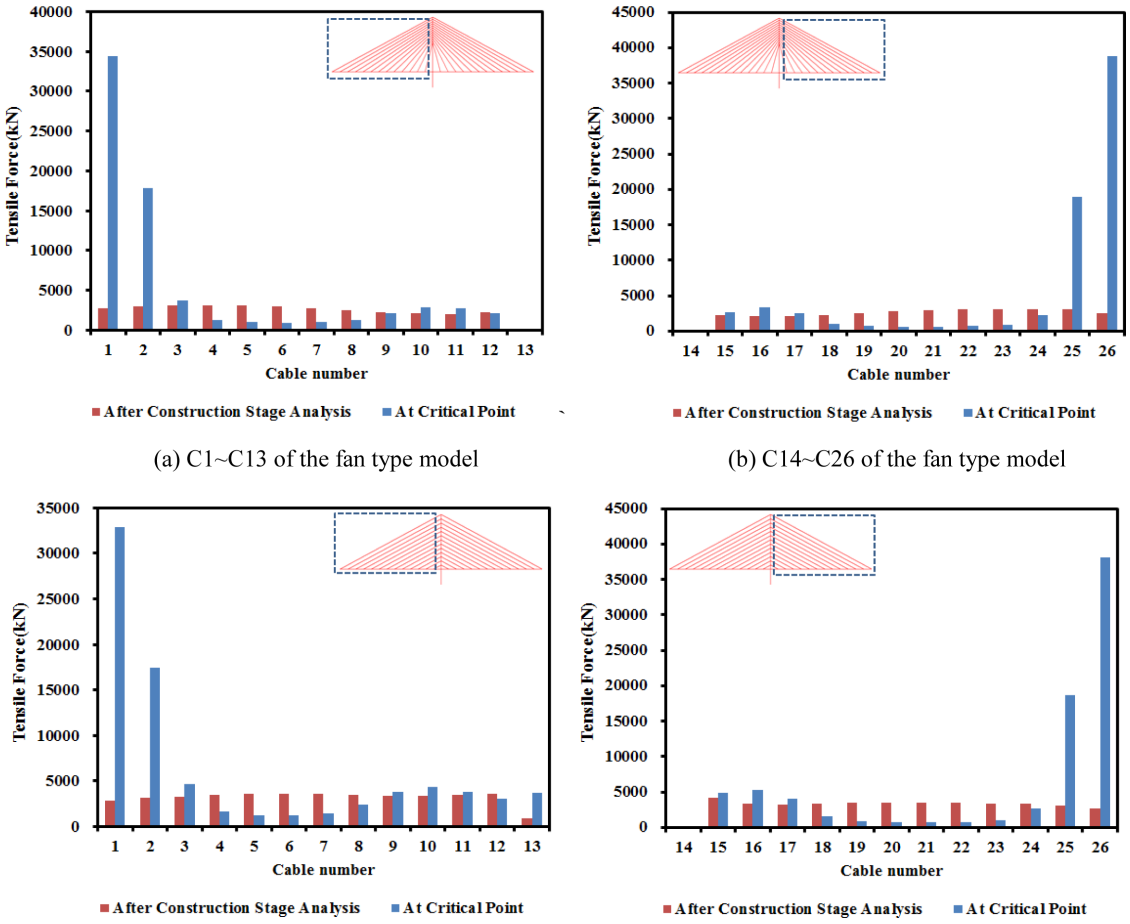

(a) C1~C13 of the fan type model

(b) C14~C26 of the fan type model

(c) C1~C13 of the harp type model

(d) C14~C26 of the harp type model

Figure 34. Tensile force distribution in the girder buckling mode (girder-mast stiffness ratio: 30).

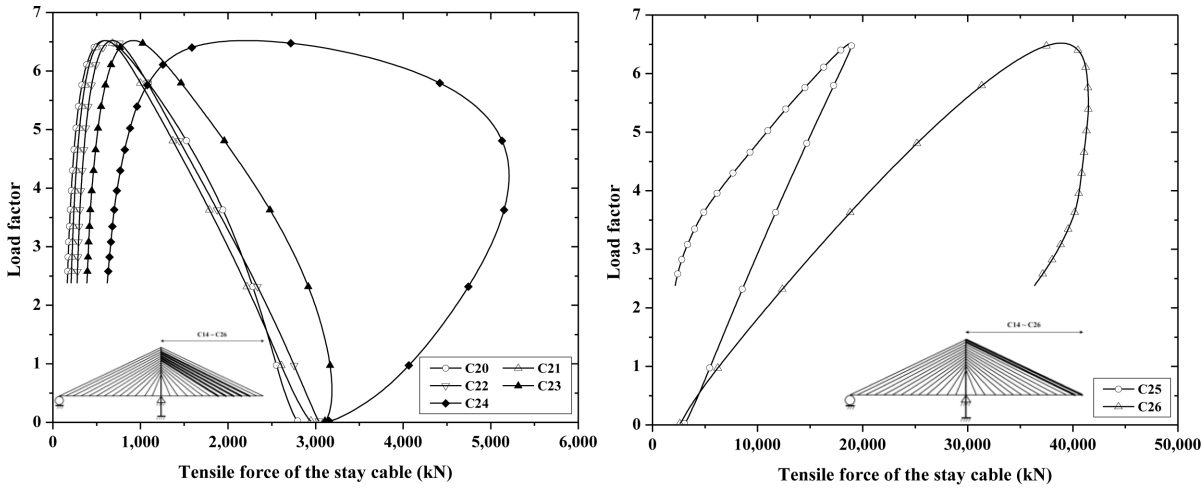

(a) C20~C24

(b) C25 and C26

Figure 35. Load-cable force curve of the fan type model (Girder-stiffness ratio: 30.0).

increase in the sag effect of the cable. In girder-mast interactive buckling, weight and sag effect increase of the cable affects the change of critical load factor more than the increase of elastic stiffness of the cable, because the mast also buckles in this buckling mode. In other words, buckling load in this buckling mode is very sensitive to the cable area, because the weight of the cable is also applied to the mast as compressive force.

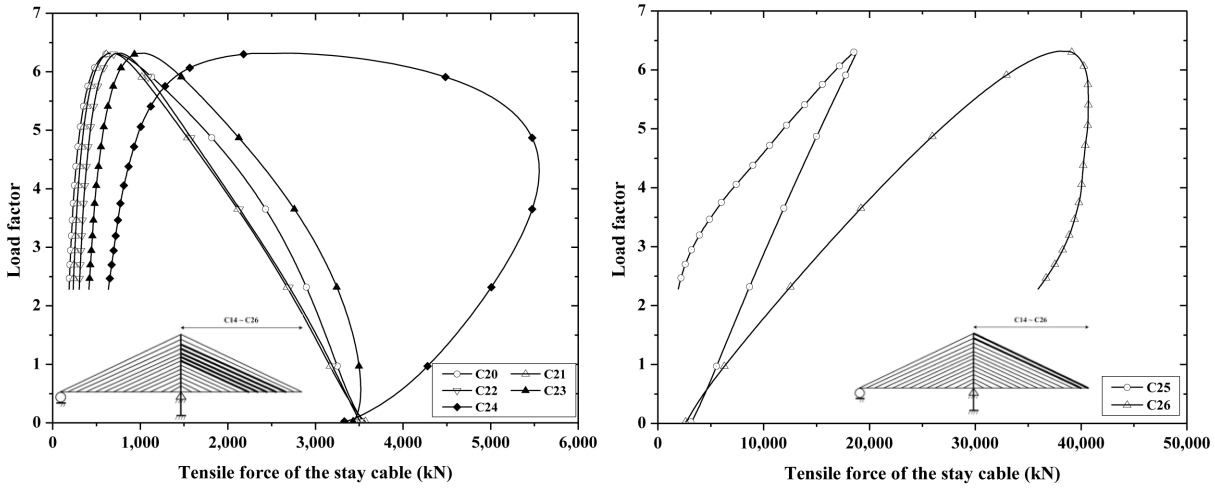

(a) C20~C24 (b) C25 and C26

Figure 36. Load-cable force curve of the harp type model (Girder-stiffness ratio: 30.0).

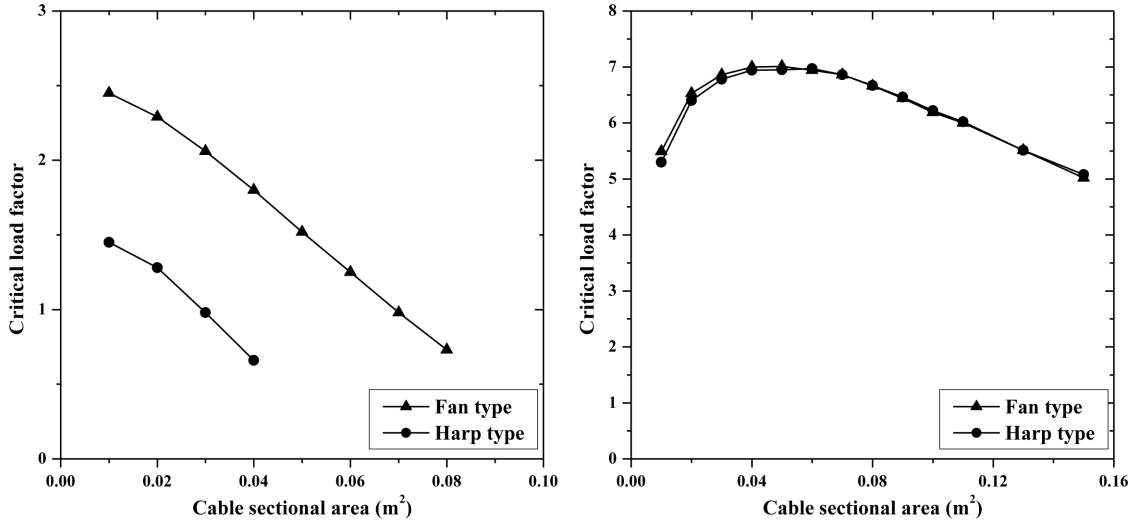

(a) Girder-mast stiffness ratio: 2.0 (b) Girder-mast stiffness ratio: 50.0

Figure 37. Critical load factor vs. cable area.

In the girder buckling mode, there is a peak point for the critical load factor. The graph can be divided into two parts. The first part shows the increase of critical load factor as the cable area increases; it can be said that the increase of elastic stiffness affects the structural stability more than the increase of the weight and sag effect of the cable. The second part shows the decrease of critical load factor as the cable area increases; the contrary can then be said.

In summary, there is a minimum required mast stiffness and optimum cable area that may lead to extreme structural stability of cable-stayed bridges under construction. As mentioned before, the girder buckling mode becomes the governing buckling mode of cable-stayed bridges under construction, when the mast has sufficient flexural stiffness. In this buckling mode, the critical load factor converges to a specific value, as the flexural stiffness of the mast increases. Moreover, there is an optimum cable area that gives the critical load factor a maximum value in this buckling mode. Therefore, when cable-stayed bridges are designed, their structural stability under construction, as well as the completed structure, should be considered and thoroughly studied. This can be achieved by rational stability analysis like the analysis method proposed in this study.

5. Conclusion

In this study, the characteristics of structural stability of cable-stayed bridges under construction were investigated. A rational structural stability analysis for cable-stayed bridges under construction was suggested, based on the

theory of nonlinear finite element analysis. Performing the proposed elastic buckling analysis using the program developed in this study, typical buckling modes were classified into two categories depending on the location of a critical member or members as follows:

(1) Interactive buckling mode
(2) Girder buckling mode.

By intensive analytical study, the effects of girder-mast stiffness ratio, cable arrangement type, and cable area on the structural stability of cable-stayed bridges under construction were investigated. According to the analytical study, the girder-mast stiffness ration mainly affects to the governing buckling modes of the cable-stayed bridges under construction. By this parametric study considering the stiffness ratios, the buckling mode changes from interactive buckling mode to girder buckling mode as the girder-mast stiffness ratio increases. Also, it was found that there are minimum required girder-mast stiffness ratios for preventing the interactive buckling mode which shows mast buckling. In addition, the effect of the sectional area of stay cables was investigated. According to this study, buckling load decreases when the area of stay cables increases in the interactive buckling mode. In this case, increase of the weight and sag effect significantly affects to the buckling load of the structures although the elastic stiffness of stay cables increases. In the girder buckling mode, the analytical results clearly show that there are optimum cable areas for maximizing the buckling load and structural stability under construction. Therefore, when cable-stayed bridges are designed, their structural stability under construction should be considered and thoroughly studied considering the effects of the girder-mast stiffness, cable arrangement type, and area of stay cables as well as other geometric conditions.

In this study, the effects of the geometric nonlinearities on the structural stability of the cable-stayed bridges under construction were mainly studied. In addition, extensive analytical research about the ultimate behavior of cable-stayed bridges under construction will need to be performed, to consider material nonlinearities, as well as various geometric nonlinearities.

Acknowledgments

This research was supported by Basic Science Research Program through the National Research Foundation of Korea (NRF) funded by the Ministry of Education (No. 2016R1D1A1A02937083).

References

Adeli, H. and Zhang, J. (1994). "Fully nonlinear analysis of composite girder cable-stayed bridges." *Computers & Structures*, 54(2), pp. 267-277.

Chen, D. W., Au, F. T. K., Tham, L. G., and Lee, P. K. K. (2000). "Determination of initial cable forces in prestressed concrete cable-stayed bridges for given design deck profiles using the force equilibrium method." *Computers & Structures*, 74, pp. 1-9.

Cheng, J. and Xiao, R. C. (2004). "Probabilistic determination of initial cable forces of cable-stayed bridges under dead loads." *Structural Engineering and Mechanics*, 17(2), pp. 267-279.

Ernst, H. J. (1965). "Der e-modul von seilen unter berucksichtigung des durchanges." *Der Bauingenieur*, 40, pp. 52-55 (in German).

Fleming, J. F. (1979). "Nonlinear static analysis of cable-stayed bridges." *Computers & Structures*, 10, pp. 621-635.

Freire, A. M. S., Negrao, J. H. O., and Lopes, A.V. (2006). "Geometric nonlinearities on the static analysis of highly flexible steel cable-stayed bridges." *Computers & Structures*, 84, pp. 2128-2140.

Gimsing, N. J. (1983). Cable supported bridges Concept & Design 2nd Edition. John Wiley & Sons Ltd., New-York.

GS E&C (2003). Development of analysis and design system for cable-stayed bridges, Research Report, Seoul, Korea.

Kim, K. S. and Lee, H. S. (2001). "Analysis of target configurations under dead loads for cable-supported bridges." *Computers & Structures*, 79, pp. 2681-2692.

Kim, S., Won, D. H., Lee, K., and Kang, Y. J. (2015). "Structural Stability of Cable-stayed Bridges." *International Journal of Steel Structures*, 15(3), pp. 743-760.

Lee, K., Kim, S., Choi, J. H., and Kang, Y. J. (2015). "Ultimate behavior of cable stayed bridges under construction: Experimental and analytical study." *International Journal of Steel Structures*, 15(2), pp. 311-318.

Lim, N. H., Han, S. Y., Han, T. H., and Kang, Y. J. (2008). "Parametric study on stability of continuous welded rail track -ballast resistance and track irregularity-." *International Journal of Steel Structures*, 8(3), pp. 171-181.

Reddy, P., Ghaboussi, J., and Hawkins, N. M. (1994). "Simulation of construction of cable-stayed bridges." *Journal of Bridge Engineering*, ASCE, 4(4), pp. 249-257.

Ren, W. X. (1999). "Ultimate behavior of long-span cable stayed bridges." *Journal of Bridge Engineering*, ASCE, 4(1), pp. 30-36.

Shu, H. S. and Wang, Y. C. (2001). "Stability analysis of box-girder cable-stayed bridges." *Journal of Bridge Engineering*, ASCE, 6(1), pp. 63-68.

Song, M. K., Kim, S. H., and Choi, C. K. (2006). "Enhanced finite element modeling for geometric non-linear analysis of cable-supported structures." *Structural Engineering and Mechanics*, 22(5), pp. 575-597.

Song, W. K. and Kim, S. E. (2007). "Analysis of the overall collapse mechanism of cable-stayed bridges with different cable layouts." *Engineering Structures*, 29, pp. 2133-2142.

Tang, C. C., Shu, H. S., and Wang, Y. C. (2001). "Stability analysis of steel cable-stayed bridge." *Structural Engineering and Mechanics*, 11(1), pp. 35-48.

Wang, P. H., Tang, T. Y., and Zheng, H. N. (2004). "Analysis of Cable-stayed Bridges during Construction by

Cantilever Methods." *Computers and Structures*, 82, pp. 329-346.

Wang, P. H., Tseng, T. C., and Yang, C. G. (1993). "Initial shape of cable stayed bridge." *Computers & Structures*, 47(1), pp. 111-123.

Wang, P. H. and Yang, C. G. (1993). "Parametric studies on cable stayed bridges." *Computers & Structures*, 60(2), pp. 243-260.

Xi, Y. and Kuang, J. S. (1999). "Ultimate load capacity of cable-stayed bridges." *Journal of Bridge Engineering*, ASCE, 4(10), pp. 14-22.

Yang, Y. B. and Kuo, S. R. (1994) Theory and analysis of nonlinear framed structures. Prentice-Hall, Inc., Singapore.

Yun, G. J. and Lee, W. S. (2001). "Nonlinear static analysis and initial shape determination analysis of cable stayed bridges", *Journal of Korean Society of Civil Engineers*, 21(1A), pp. 165-177. (in Korean)